Determining Momentum and Energy Corrections for g1c Using Kinematic Fitting

Mike Williams, Doug Applegate and Curtis A. Meyer

Carnegie Mellon University

June 7, 2004

Abstract

We have used the CLAS Kinematic Fit and the exclusive reaction $\gamma p \to p\pi^+\pi^-$ to derive energy and momentum corrections for the g1c run period. By selectively leaving particles out of the fit, and then comparing fit and measured quantities, we have been able to derive corrections for the photon energy and the final state particles.

Contents

1 Introduction

In late 2003, a Kinematic Fitting package for the CLAS experiments was released by the authors. The details of this package can be found in an earlier CLAS-Note [1], and background information on the mathematics of the fitting procedure are described in a book by Brandt [2]. The purpose of this study was to understand what if any momentum and energy corrections should be applied to the data from g1c.

2 The Procedure

The $\gamma p \to p\pi^+\pi^-$ data set is an excellent environment in which to study the CLAS detector. The reaction is fully reconstructed, which in turn allows one to carry out a 4-constraint (4-C) fit to the data. The pull [3] and confidence-level distributions from this data can then point one in the correct direction to small problems in the data set. These small systematic errors can then be studied in detail by selectively leaving out particles in a series of 1-C fits performed on the data.

This study started by examining the momentum resolution of the π^- by using the reaction:

$$\gamma p \to p\pi^+(\pi^-)_{missing}.$$

Treating the π^- as an undetected particle in a 1-C fit yields a momentum, $\vec{p}_{\pi^-(fit)}$, that is not biased by the measured value. The difference,

$$\Delta\vec{p}_{\pi^-} = \vec{p}_{\pi^-(fit)} - \vec{p}_{\pi^-(meas)} \tag{1}$$

can then be studied as a function of pion angles, momentum and sector number. Following this work, the π^- is corrected, and one can then study the correction to the π^+ momentum. Because of the asymmetric bending of positive and negative particles, these two corrections are not expected to be the same. With this complete, the proton is examined. While we nominally expect the proton and the π^+ corrections to be the same, there may be residual issues in the energy loss corrections of protons versus pions that introduce small differences. All energy loss corrections are performed using the ELOSS [6] package and are performed before any fits or comparisons. Finally, we can look at the deviation in the tagged photon energy. This process can then be iterated to obtain the best set of corrections. We note here that the changes to the ELOSS corrections along with the corrections to the tagged photon energy were found to be significant enough to warrant restarting the process with first approximations for these already inserted. The results presented in the following sections were obtained from the final iteration.

As a reference point, we present the confidence-level and pull distributions obtained by performing a 4-C fit on the data prior to making any of the corrections presented in this paper (standard ELOSS corrections have been made). Figure 1 shows the confidence level distribution, while Figure 2 shows the pull distributions, the means and widths of the pull distributions are given in Table 1. Both the confidence level and pull distributions look quite reasonable, while it could be argued that some of the pulls are skewed, they are within acceptable limits for carrying out kinematic fits.

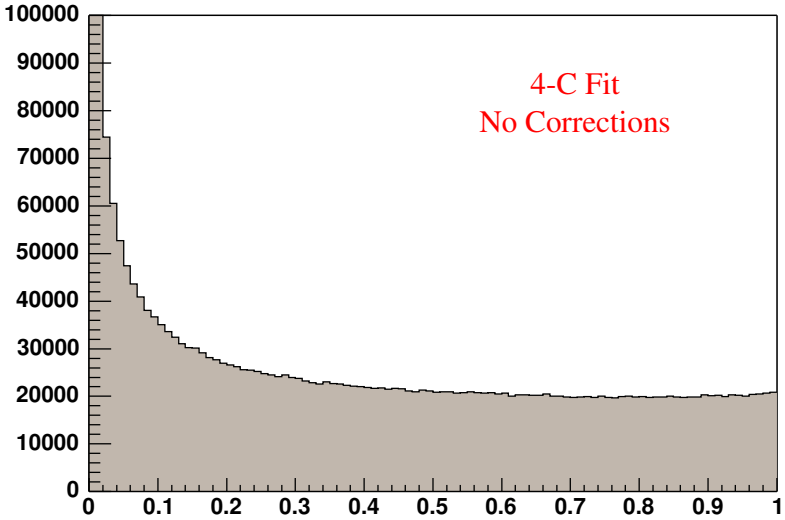

Figure 1: The confidence level distribution for the 4-C fit to $\gamma p \rightarrow p\pi^+\pi^-$ before any momentum corrections have been made(standard ELOSS corrections have been made).

Quantity	Mean	Sigma
p_p	0.208	0.963
λ_p	-0.025	0.944
ϕ_p	0.125	0.965
$p_{\pi+}$	0.094	0.972
$\lambda_{\pi+}$	-0.028	1.016
$\phi_{\pi+}$	-0.041	1.031
$p_{\pi-}$	0.033	0.999
$\lambda_{\pi-}$	-0.011	1.003
$\phi_{\pi-}$	-0.061	1.058
E_γ	-0.201	1.019

Table 1: The means and widths of the pull distributions, shown in Figure 2, before momentum corrections have been applied to the data.

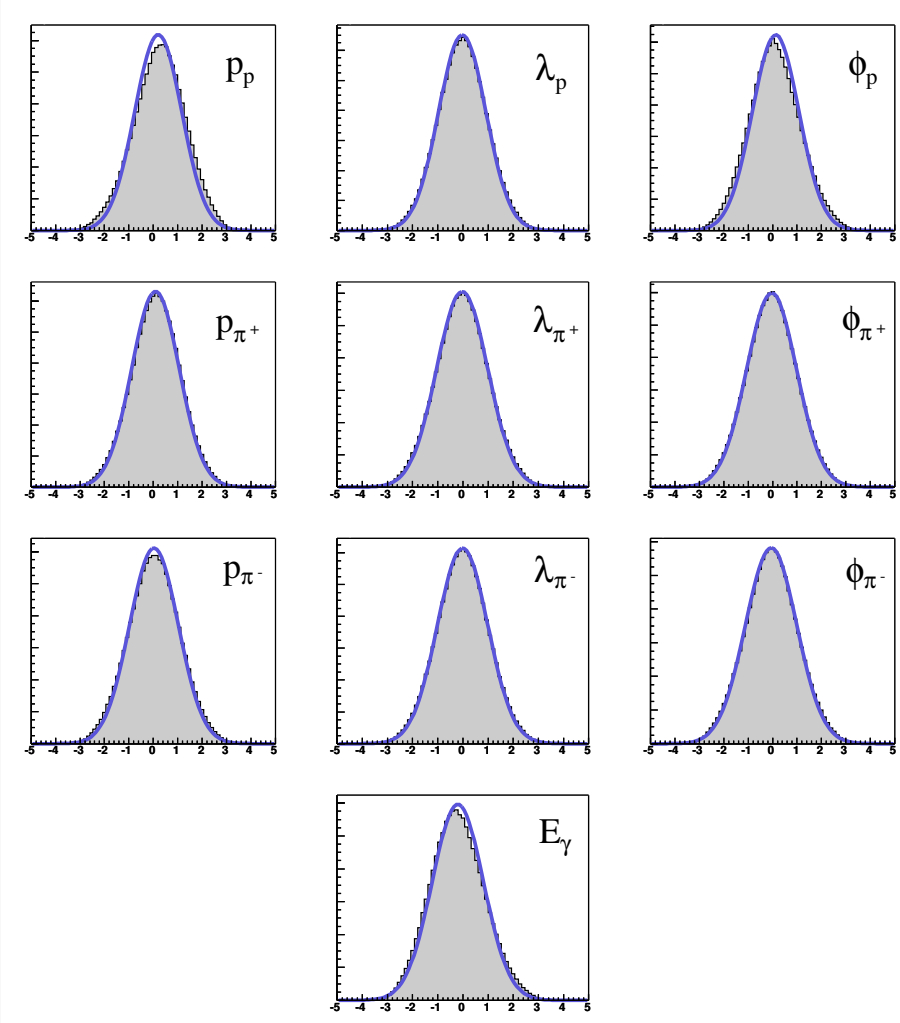

Figure 2: The pull distributions for the 4-C fit to $\gamma p \to p\pi^+\pi^-$ before any momentum corrections have been made. The pulls have been fit with a Gaussian function which is overlaid as the solid line. The means and σ's are given in Table 1.

2.1 The π^- Spectrum

When the π^- is treated as a missing particle in a 1-C fit, we can form the quantity $\Delta\vec{p}_{\pi^-}$ (see Eq. 1). To get an idea of where problems might be, we made 2-D histograms of Δp vs. p, θ and ϕ, then fit each bin to a gaussian and plotted the means. Figure 3 shows the mean of this difference as a function of the π^- momentum, while Figures 4 and 5 show it as a function of θ and ϕ respectively. One striking feature seen in all of these plots is the large offset in sector 2 relative to the other 5 sectors in CLAS. Figure 4 shows that this appears to be concentrated at forward angles (θ), and that the deviation can get as large as $30\,MeV/c$. All other sectors show a significantly smaller deviation. This effect was actually first observed by Kim [4] and is attributed to an alignment issue in the Region-3 drift chambers. Clearly any corrections that we make are going to have to be sector dependent. It is also clear that the corrections have an apparent complicated dependence on θ, ϕ and p, something noted by Taylor [5].

Rather than trying to correct the momentum in terms of its' magnitude, p, we chose to use the quantity which is actually measured, $\frac{Bdl}{p}$, where $Bdl \equiv |\int \vec{B} \times d\vec{l}\,|$ is the total amount of magnetic field the particle travels through in CLAS. This dependence was seen in earlier work by Kim [4]. The quantity Bdl is computed by crudely swimming the particles through the CLAS magnetic field. Figure 6 shows a plot of the result of several of these tracks.

We can then correct $\frac{Bdl}{p}$ by dividing each sector up into 10 ϕ bins giving us a correction of the form,

$$\Delta\frac{Bdl}{p} = \alpha_{ij} + \beta_{ij}\frac{Bdl}{p} \tag{2}$$

$$\Delta\frac{Bdl}{p} = a_i + b_i\theta + c_i\theta^2 + d_i\theta^3 + e_i\theta^4 \tag{3}$$

where $i = 1, 2, .., 6$ is the sector number and $j = 1, 2, ...10$ is the ϕ bin. The parameters α, β, a, b, c, d and e are constants which are fit to the available data. Terms where $\Delta\frac{Bdl}{p}$ depends only on θ, ϕ and sector number are due to drift chamber misalignments. Thus, Equation (3) can be interpreted as the θ-dependence of the misalignments, while α_{ij} in Equation (2) can be interpreted as the ϕ-dependence of the misalignments averaged over all θ. The term $\beta_{ij}\frac{Bdl}{p}$ in Equation (2) accounts for problems in calculating $\int \vec{B} \times d\vec{l}$ that could be caused either by inaccuracies in the CLAS magnetic field map or by drift chamber misalignments leading to systematic shifts in the particles' trajectories with respect to the field map.

Figures 18-23 in Appendix A show the results of plotting $\Delta\frac{Bdl}{p}$ vs. $\frac{Bdl}{p}$, dividing each sector into 10 ϕ bins, for the π^-. Each bin is, to first order, linear in $\frac{Bdl}{p}$ as expected. We fit each bin to Equation(2), then apply this correction and plot $\Delta\frac{Bdl}{p}$ vs. θ for each sector (see Figure 24 in Appendix A). We do not correct the measured angles θ and ϕ. We found the systematic shifts in these angles to be less than $1mrad$, which is not enough to pose any problems during the kinematic fitting process.

It is important to keep in mind that EXCEPT for some forward angle regions in sector 2, the typical size of these momentum corrections are a few MeV. These are **NOT** large corrections. Figure 17 shows the corrections to the π^- momentum as a function of p, θ and ϕ respectively summed over all sectors.

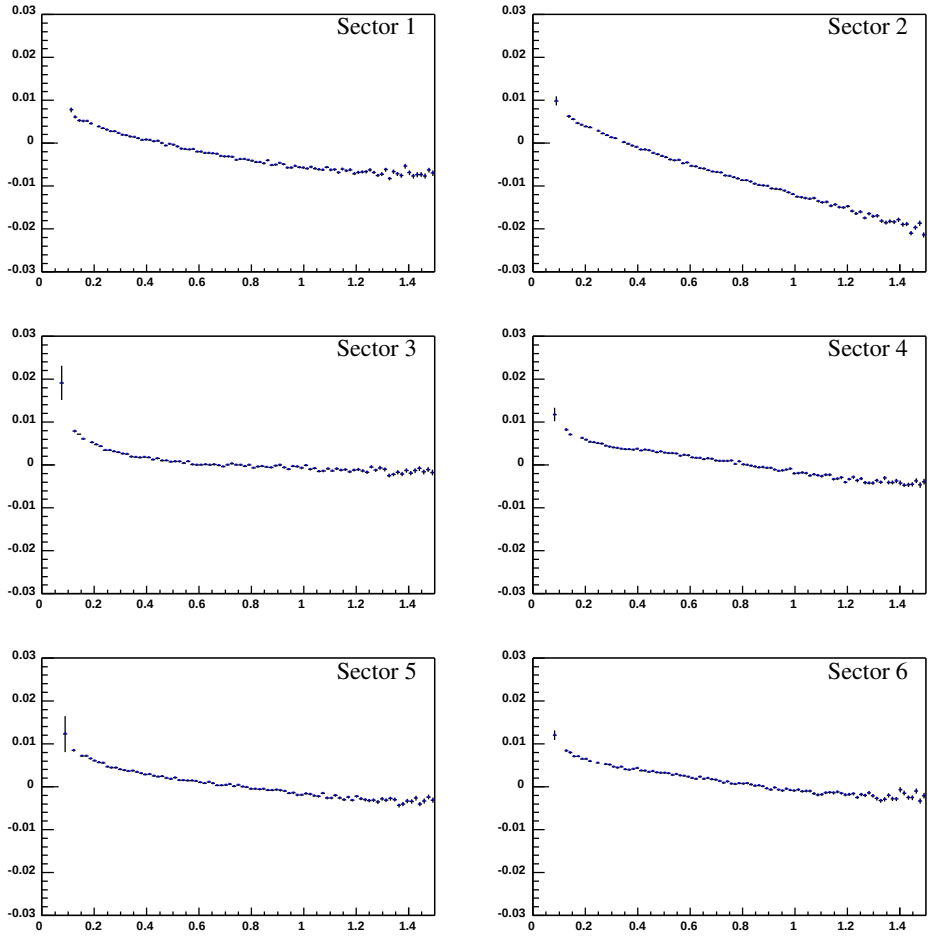

Figure 3: Δp vs. p: The change in momentum of the π^- as a function of the π^- momentum for each of the six sectors in the CLAS detector.

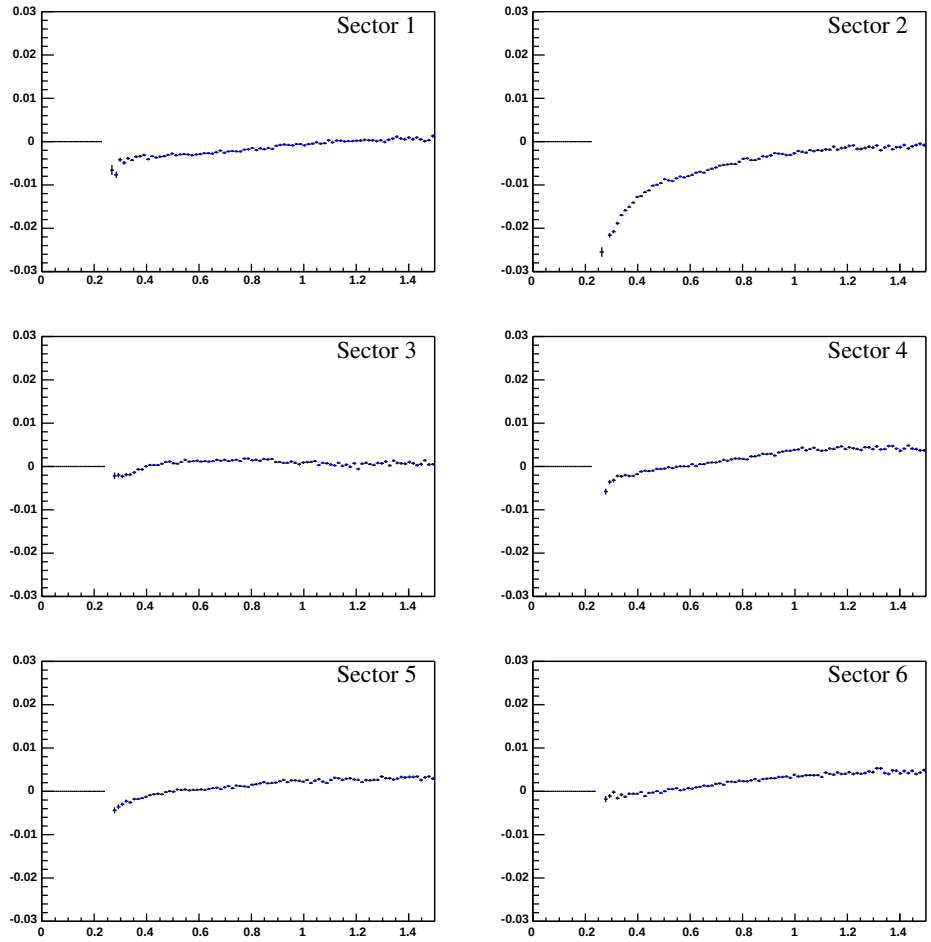

Figure 4: Δp vs. θ: The change in momentum of the π^- as a function of the π^- θ angle for each of the six sectors in the CLAS detector.

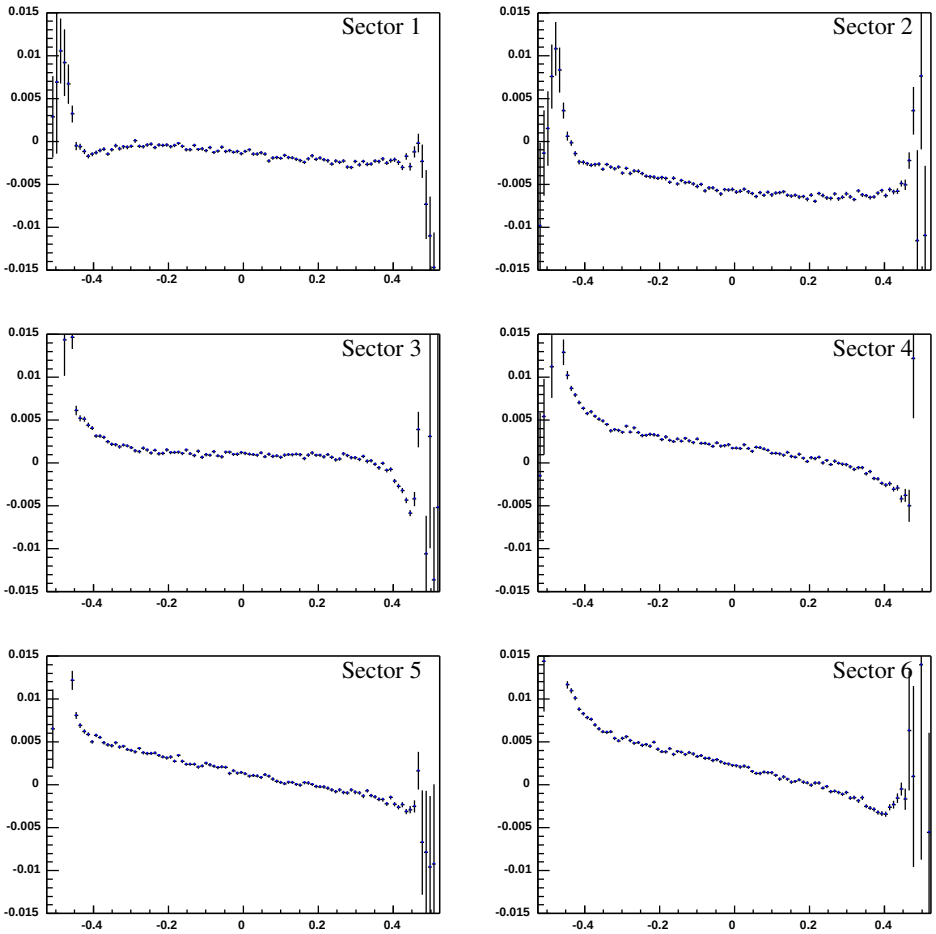

Figure 5: Δp vs. ϕ: The change in momentum of the π^- as a function of the π^- ϕ angle for each of the six sectors in the CLAS detector.

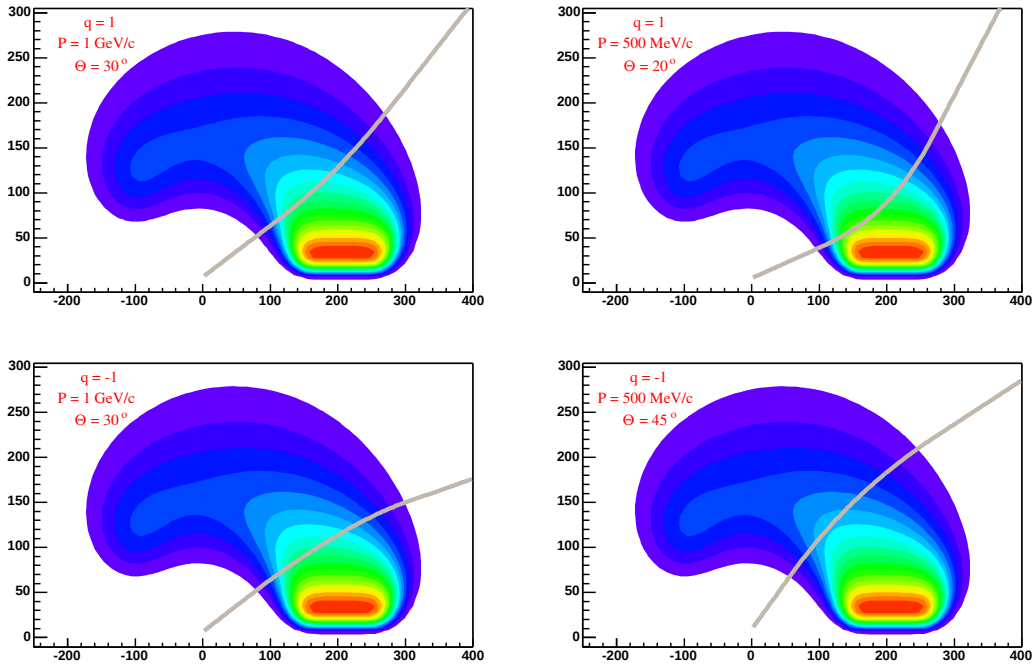

Figure 6: Output of the mini tracking to compute the $\int \vec{B} \times d\vec{l}$ along a particle trajectory through the magnetic field.

2.2 The π^+ spectrum

We followed the same procedure for the π^+ as we did for the π^-. We treated the π^+ as the missing particle in a 1-C fit and used the quantity $\Delta\frac{Bdl}{p}$ to determine the corrections to the magnitude of the π^+ momentum. Figures 26-31, in Appendix B show the results of plotting $\Delta\frac{Bdl}{p}$ vs. $\frac{Bdl}{p}$, dividing each sector into 10 ϕ bins, for the π^+. Each bin is, to first order, linear in $\frac{Bdl}{p}$ just as for the π^-. We fit each bin to Equation(2), then apply this correction and plot $\Delta\frac{Bdl}{p}$ vs. θ for each sector (see Figure 32 in Appendix B).

Again, except for some forward angle regions in sector 2, the typical size of these momentum corrections are a few MeV. Figure 25 shows the corrections to the π^+ momentum as a function of p, θ and ϕ respectively summed over all 6 sectors.

2.3 The p spectrum

If all of the problems in the measured momentum are due to either magnetic field or alignment issues in CLAS, then one would expect that the corrections for all positive particles (π^+, K^+ and p) would be the same, and all corrections for negative particles, (π^- and K^-) will be the same. Initially, we were seeing differences between p and π^+. However, we soon realized that it appeared the ELOSS corrections were still somewhat too small. In Figure 7 we show the ELOSS correction (Δp) as a function of the particle momentum for the proton. Figure 8 shows the correction to ELOSS needed on the proton as a function of the size of the applied correction. The corrections needed are linear with sector dependent slopes corresponding to about 18%. We attribute this additional correction to energy loss in traversing the tracking region of CLAS. Note that this is only really relevant for low momentum ($< 300\,MeV/c$) protons. If we apply these sector dependent scale factors to the ELOSS package corrections, then the corrections that we derived for the π^+ in the previous section also work for the protons. Thus, our corrections depend only on which sector in CLAS the particle traveled through and the particle's charge. This is consistent with our picture of how these corrections should work.

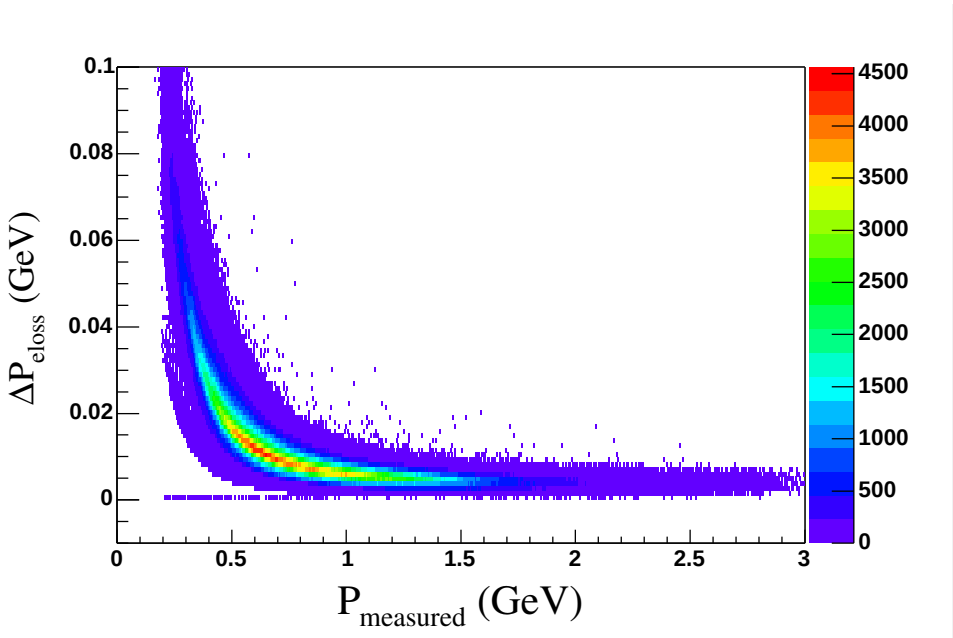

Figure 7: *Eloss Correction* vs. p : Correction applied to the magnitude of the proton momenta by the ELOSS package.

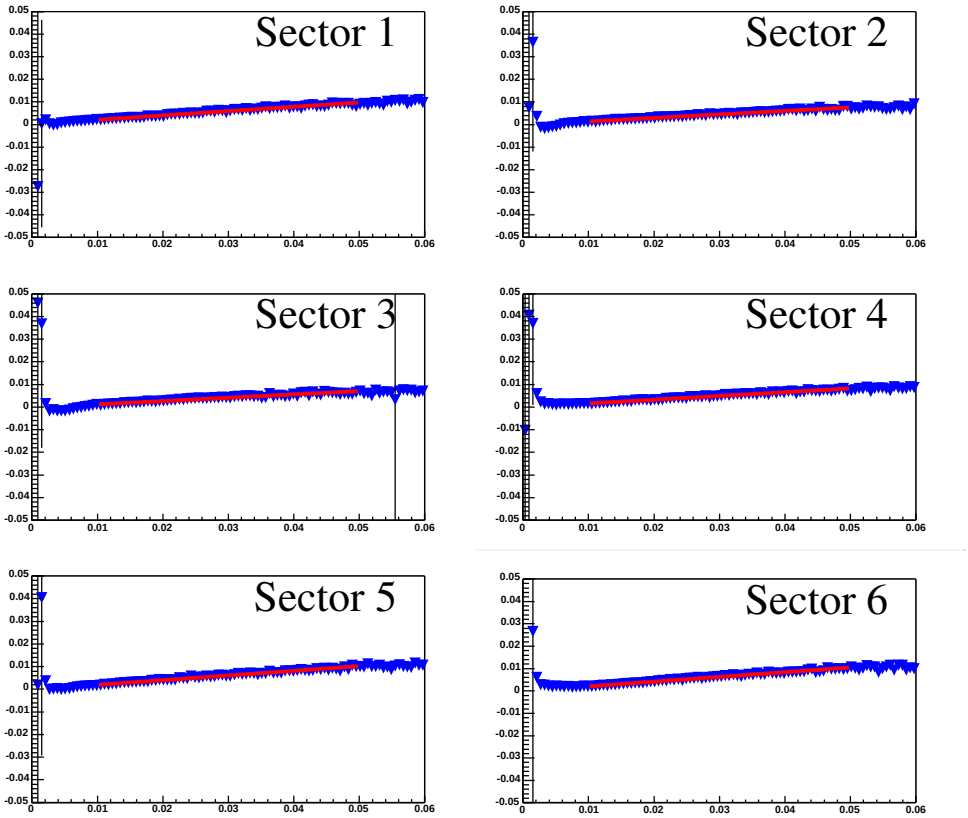

Figure 8: ΔP vs. *Eloss Correction* : Correction needed for the proton momentum, $after$ the π^+ momentum corrections and standard ELOSS corrections have been made, versus the energy loss correction obtained from the ELOSS package.

Sector	ELOSS Scale Factor
1	1.192
2	1.156
3	1.146
4	1.166
5	1.206
6	1.212

Table 2: . Scale Factors this analysis shows need to be applied to the energy loss corrections obtained from the ELOSS package.

2.4 The Photon Beam Energy

In the final round of analysis, all final state particles in the detector have had their momentum corrected, and we then want to look at the measured photon energy. Because it is not trivial to modify the kinematic fit to leave the photon energy free, we took a somewhat different approach here. We have used the target mass and the detected final state particles to predict what the photon beam energy, $E_{\gamma(fit)}$, should be and then compared it to the measured energy, $E_{\gamma(measured)}$. So $E_{\gamma(fit)}$ is defined as,

$$E_{\gamma(fit)} = E_p + E_{\pi^+} + E_{\pi^-} - m_p. \tag{4}$$

We can then form the difference:

$$\Delta E_\gamma = E_{\gamma(fit)} - E_{\gamma(measured)}. \tag{5}$$

To obtain a correction for the photon energy, we first histogrammed ΔE_γ vs. E_γ. We then fit each bin of this histogram to a Gaussian then plotted the mean versus the photon energy. Figure 9 shows this histogram fitted to a piecewise quadratic function in E_γ. It is interesting that this function is not constant. The double hump structure is similar in shape to the results of Stepanyan [7]. (As an aside, there is an absolute offset between the values in this study and those of Stepanyan). Since this observation, the shift can be explained by a calculable sage in the tagger [9].

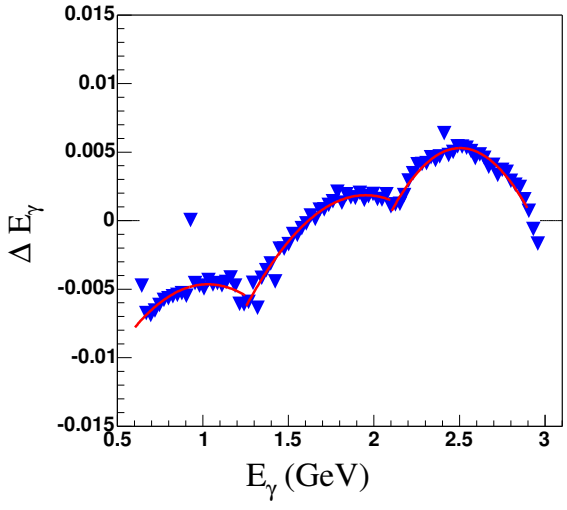

Figure 9: Correction to the tagged photon beam energy as a function of the beam energy.

3 Comparison of Results

After all of the corrections described in this note have been performed, the resulting confidence-level is shown in Figure 10. Clearly, some of the errors going into the fit were slightly too large. A result that should be expected from the fact that we have corrected 4 of the 10 measured quantities. In our earlier work [1], the errors on the energy-loss were fit to the data. After this study, we refit those and come up with numbers that are about 60% of the earlier error. After we have adjusted the errors to compensate, the resulting confidence level distribution is shown in Figure 11 and the pull distributions are shown in Figure 12. The means and σ's of the pull distributions are shown in Table 3. It should be noted that the error that we adjusted is only one of several components that feed into the total error. The effect on the total error is much smaller than implied by the 60% number, but it is the one degree of freedom that is not a-priori totally constrained by physics.

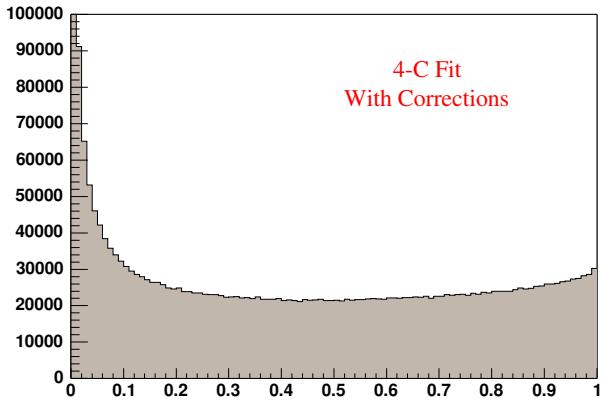

Figure 10: The confidence level distribution for the 4-C fit to $\gamma p \rightarrow p\pi^+\pi^-$ after all momentum corrections have been made. The rise near 1 demonstrates a need to scale down our errors slightly now that we've improved the data being input to the fit.

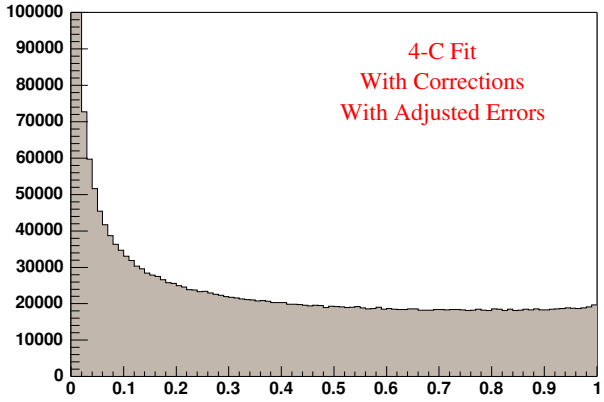

Figure 11: The confidence level distribution for the 4-C fit to $\gamma p \rightarrow p\pi^+\pi^-$ after all momentum corrections have been made and the errors have been adjusted.

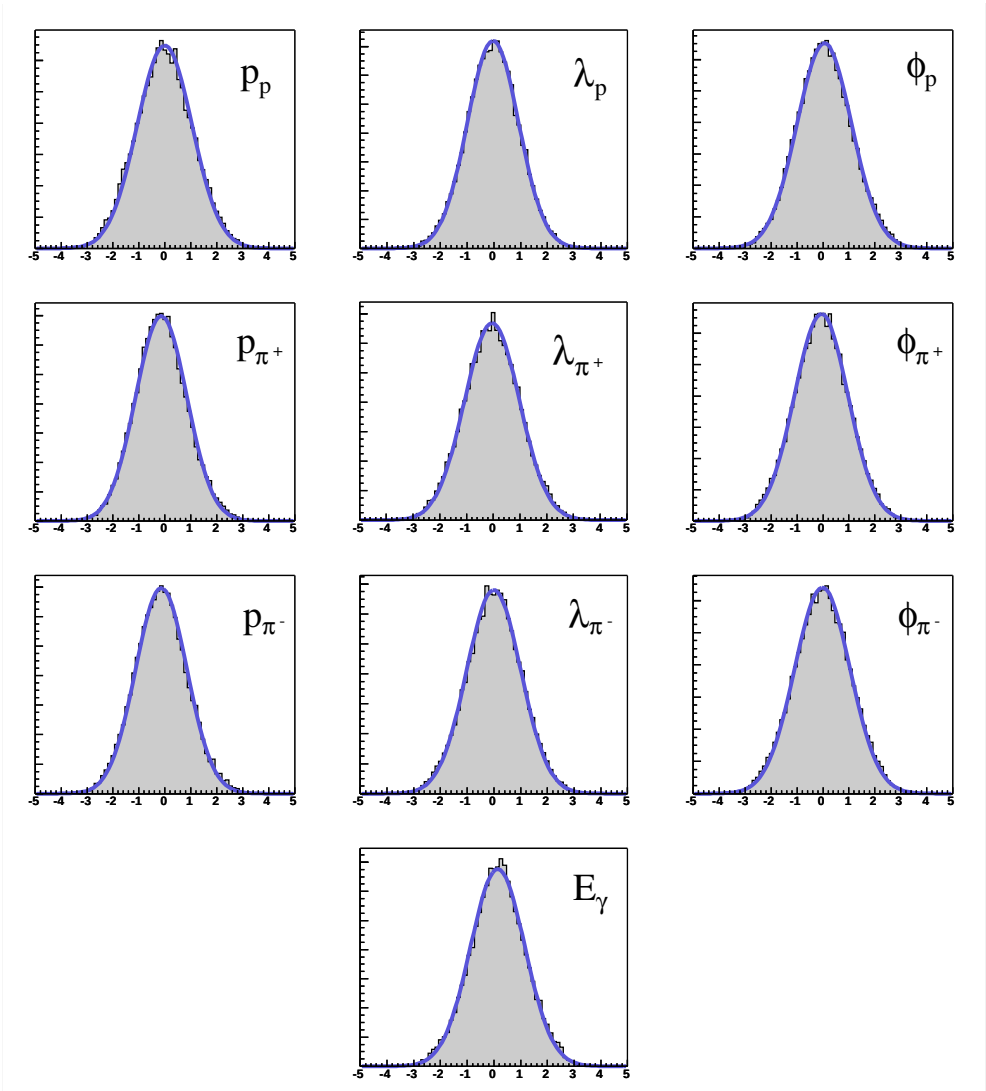

Figure 12: The pull distributions for the 4-C fit to $\gamma p \to p\pi^+\pi^-$ after all momentum corrections have been made.

Quantity	Mean(initial)	Mean (final)	Sigma(initial)	Sigma(final)
p_p	0.208	-0.022	0.963	1.011
λ_p	-0.025	-0.031	0.944	0.954
ϕ_p	0.125	0.044	0.965	0.982
p_{π^+}	0.094	0.044	0.972	0.985
λ_{π^+}	-0.028	-0.018	1.016	1.016
ϕ_{π^+}	-0.041	-0.010	1.031	1.035
p_{π^-}	0.033	0.025	0.999	1.010
λ_{π^-}	-0.011	-0.005	1.003	1.005
ϕ_{π^-}	-0.061	-0.012	1.058	1.068
E_γ	-0.201	-0.077	1.019	1.006

Table 3: The means and widths of the pull distributions before and after all momentum corrections have been applied to the data.

3.1 Mass peaks for known resonances

In order to demonstrate that the kinematic fit is robust against these small errors in the momentum and energy, we have examined the reaction:

$$\gamma p \rightarrow p\pi^+\pi^- X_{miss}. \tag{6}$$

where the missing particle can be either a π° or an η. In the case of the π°, there are two three pion resonances of interest, $\eta \rightarrow \pi^+\pi^-\pi^\circ$ and $\omega \rightarrow \pi^+\pi^-\pi^\circ$. In the case of the missing η, the main resonance of interest is the $\eta' \rightarrow \eta\pi^+\pi^-$. We select the data for display by placing a 10% confidence level cut on the 1C fit to the two channels. In Figure 13, we show the three mass peaks as produced using unfit and uncorrected momentum. This is effectively the missing mass off the $\gamma p \rightarrow pX_{miss}$ spectrum. The peaks have been fit using a Voigtian function [8] with the natural width of the resonance as an input parameter. Figure 14 shows the same spectrum after all momentum corrections have been made, but again without fitting. There is significant improvement in the accuracy of masses and a slight inprovement in the widths. In Figure 15 we show the kinematically fit spectrum starting from the uncorrected momentum, while in Figure 16 we show the fits starting from the corrected momentum. In Table 4 we summarize the results of all of these fits. It should be pointed out that the value of the fit mean can vary by about $\pm 0.25\, MeV/c^2$ due to assumptions about background shape and variations in fit ranges. Except for the case of uncorrected measured data, all of the masses are extremely accurate. The slight improvements in the width from the momentum corrections translates into a narrower resolution in the fit data as well.

Particle	Mass [10]	Uncor., Measured		Cor., Measured		Uncor., Fit		Cor., Fit	
		Mean	σ	Mean	σ	Mean	σ	Mean	σ
η	547.30	551.9	6.343	548.4	6.193	548.7	4.900	547.8	3.521
ω	782.56	782.4	6.634	782.3	6.320	782.4	5.869	782.2	5.620
η'	957.78	956.2	5.081	957.2	5.088	956.6	4.158	957.3	4.007

Table 4: The mass and widths of known resonances fit using a Voigtian function to derive the mass and resolution width. The four blocks of data correspond to uncorrected momentum using measured values, corrected measured momentum, uncorrected momentum that has been kinematically fit and corrected momentum that has been kinematically fit. All quantities are given in MeV/c^2.

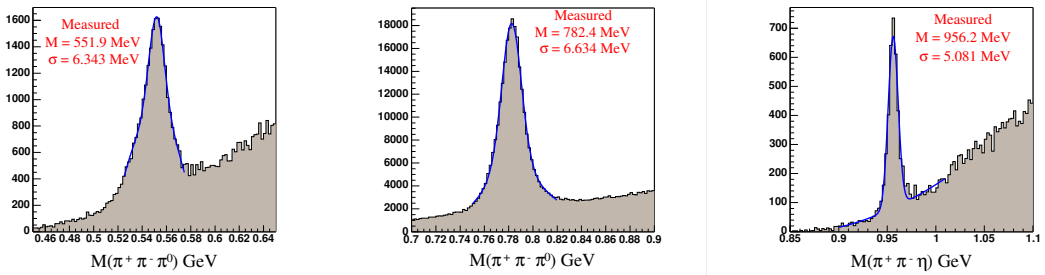

Figure 13: The invariant mass spectrum for the η (left), ω (center) and η' (right) made using the unfit and uncorrected momentum.

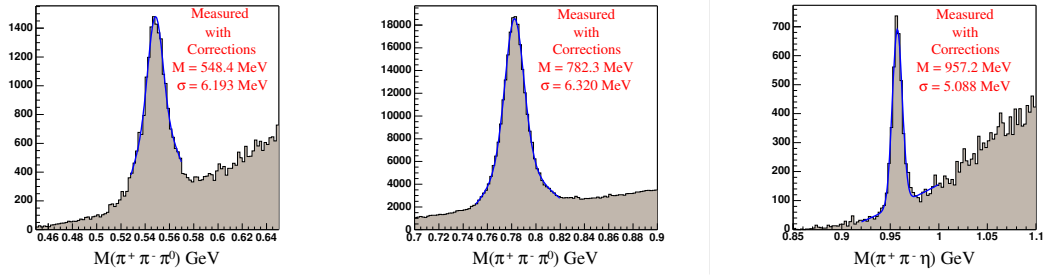

Figure 14: The invariant mass spectrum for the η (left), ω (center) and η' (right) made using the unfit but corrected momentum.

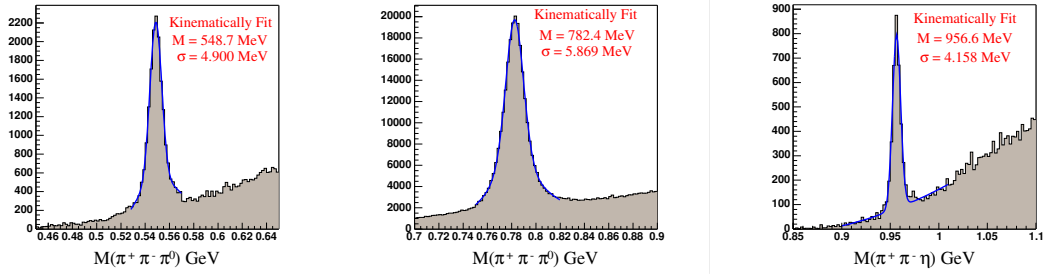

Figure 15: The invariant mass spectrum for the η (left), ω (center) and η' (right) made using the kinematically-fit uncorrected momentum.

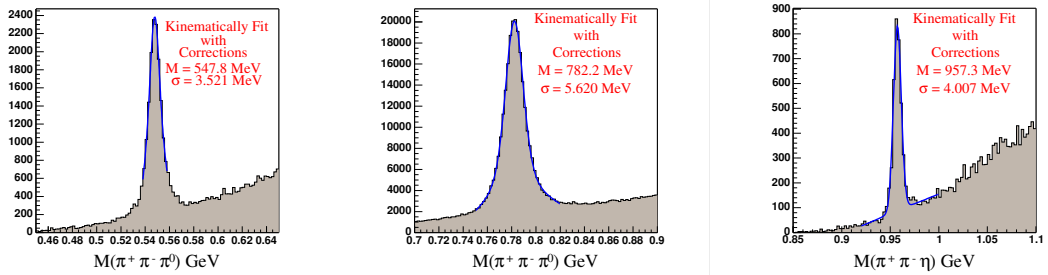

Figure 16: The invariant mass spectrum for the η (left), ω (center) and η' (right) made using the kinematically-fit and corrected momentum.

4 Summary and Conclusions

We have carried out a detailed study of momentum and energy corrections for the CLAS g1c data. The result of this work is three-fold. First, the photon beam energy needs to be corrected by the interesting function shown in Figure 9. If the slope and offset are removed from this function, the wiggles are almost certainly within the design goals of the tagger. However, using this function, we can actually improve upon that slightly. Second, we believe that the energy loss of the particles as they travel through the tracking region is not accurately handled in CLAS. We have identified a sector dependent effect that is on average about 18% of the ELOSS correction that needs to be added. This correction is needed if we want the residual momentum corrections for all particles of the same sign to be identical. Finally, we have developed residual momentum corrections for particles that depend only on the sector in CLAS and the charge of the particles. All of these functions will be checked into the CLAS CVS repository. Applying these corrections will provide improved reconstructed quantities in CLAS data.

We also point out that even before these corrections, the error functions worked out in our kinematic fit study [1] were of high enough quality that a good kinematic fit could be made. While slight improvements are achieved by applying the corrections before using a fit, they are **NOT** necessary to obtain good results kinematically fitting the data.

References

[1] Mike Williams and Curtis A. Meyer, **Kinematic Fitting in CLAS**, CLAS-Note 03-017, November 2003.

[2] Sigmund Brandt, **Statistical and Computational Methods in Data Analysis**, North Holland Publishing Company, (1970), (see Chapter 9).

[3] A. G. Frodesen and O. Skjeggestad, **Probability and Statistics in Particle Physics**, Columbia University Press, (1979), (see Chapter 10 on *stretch functions*).

[4] K. Y. Kim, H. Denizli, J. A. Mueller and S. A. Dytman, **General momentum correction form for CLAS: A study of momentum corrections for the Prod 1-9 cooking of e1c data**, CLAS-Note 01-018, October 2001.

[5] S. Taylor and G. Mutchler, **Analysis update for E89-024 (radiative decays of excited-state hyperons)**, CLAS Analysis Note 2003-108, February 2004.

[6] Eugene Pasyuk, The CLAS ELOSS Package.

[7] Stepan Stepanyan, **Evidence for an Exotic Pentaquark Baryon State $\Theta^+(1530)$, in the $\gamma d \to pK^+K^-n$ reaction**, CLAS Analysis Note 2003-105, July 2003.

[8] Curtis A. Meyer, Mike Williams and Robert Bradford, **Computing Invariant Masses and Missing Masses**, CLAS-Note 04-008, February 2003.

[9] Dan Sober, private communication.

[10] The 2002 version of the PDG.

A π^- Corrections

This appendix shows detailed plots of the π^- momentum corrections. Figures 18, 19,20,21,22 and 23 show the quantity $\Delta\frac{Bdl}{p}$ versus $\frac{Bdl}{p}$ in sectors 1-6. The plots are broken into ten bins in ϕ in each sector. Figure 17 shows the corections applied to data from one run in g1c summed over all 6 sectors. These corrections are small, typically only a few MeV.

One interesting feature of these plots is that the slope decreases as ϕ increases for each sector. We interpret this as a rotation of the drift chambers with respect to the torus coils. Thus, one side of each sector is closer to the coils while the other side is farther away than what is input to the tracking code. This results in a reported Bdl that is too large on the side of the sector rotated away from the coils and too small on the side of the sector rotated towards the coils.

While the decreasing slope with respect to ϕ is common to all sectors, the actual values of the slopes are different in each sector. One interpretation for this effect is that the current isn't the same in all six torus coils. In fact, to cause the affect that we see in the data the differences in the current would have to be $\approx 0.2\%$, or a few amps.

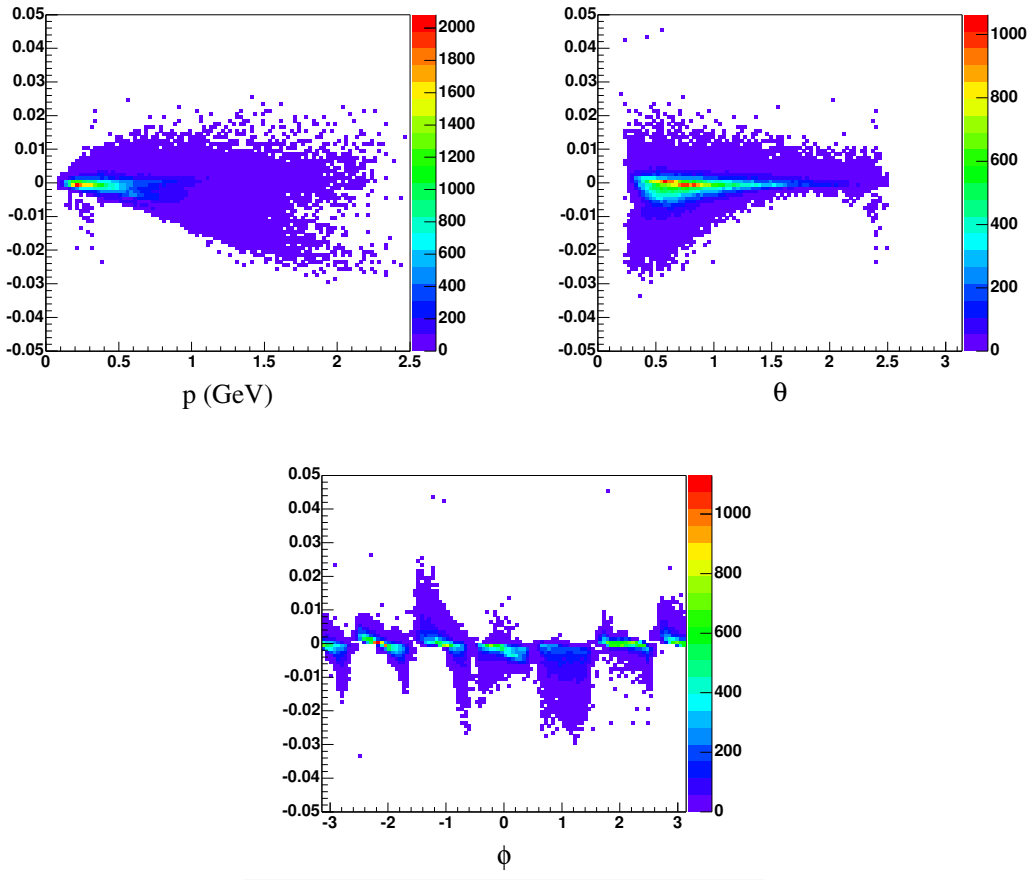

Figure 17: Corrections to the π^- momentum as a function of p, θ and ϕ summed over all 6 sectors.

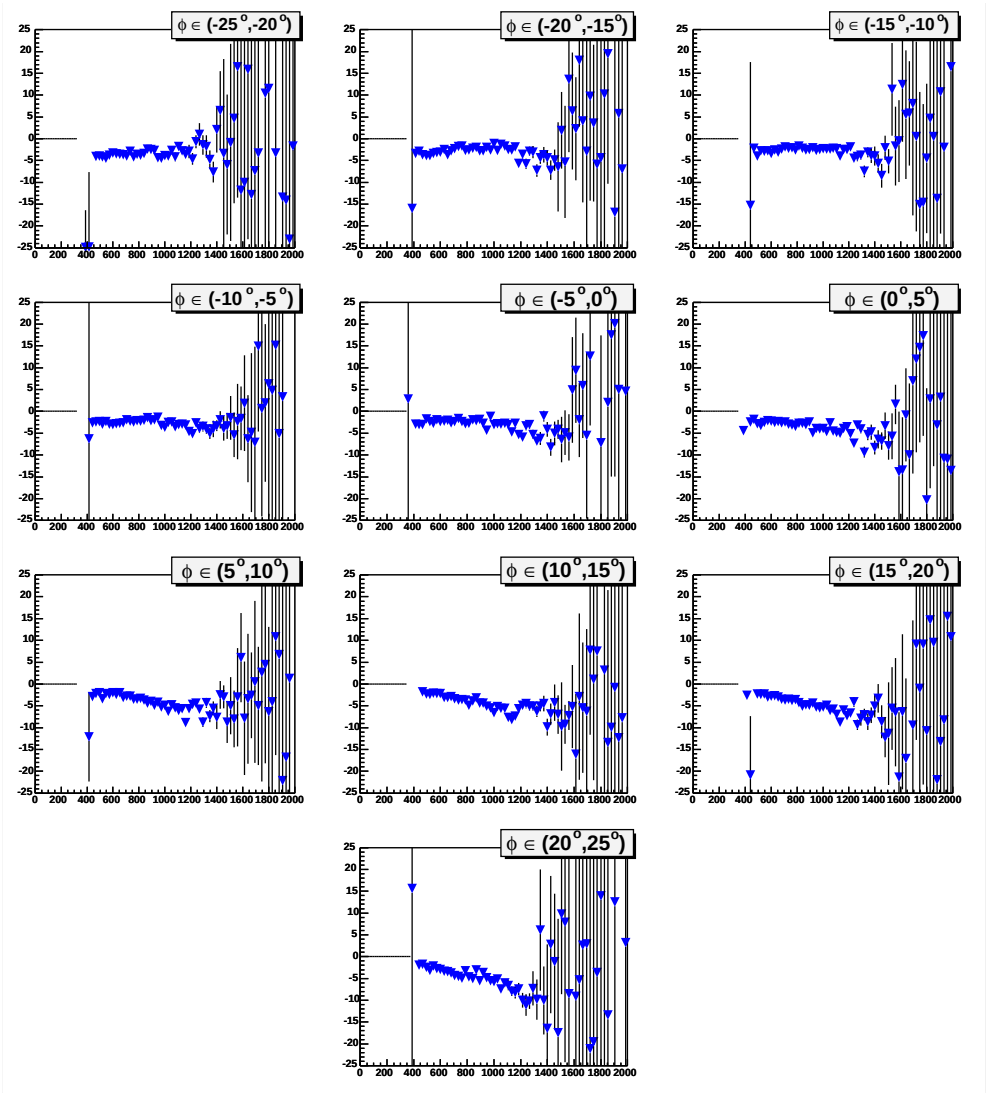

Figure 18: $\Delta\frac{Bdl}{p}$ vs. $\frac{Bdl}{p}$: The change in $\frac{Bdl}{p}$, for the π^-, in Sector 1. $\frac{Bdl}{p}$ has units of $\frac{kG\cdot cm}{GeV}$ and ϕ is the sector dependent azimuthal angle, with $\phi = 0$ corresponding to the center of the sector.

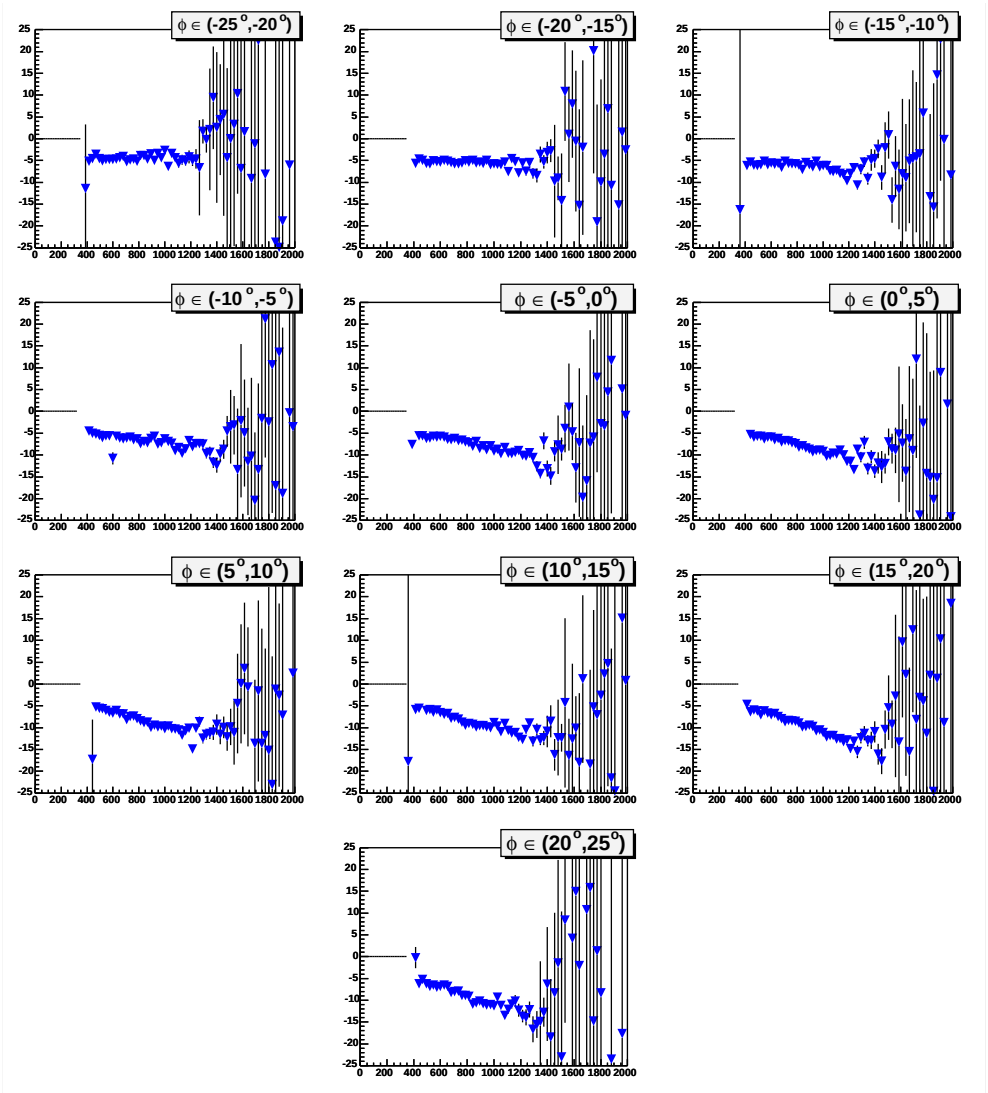

Figure 19: $\Delta\frac{Bdl}{p}$ vs. $\frac{Bdl}{p}$: The change in $\frac{Bdl}{p}$, for the π^-, in Sector 2. $\frac{Bdl}{p}$ has units of $\frac{kG \cdot cm}{GeV}$ and ϕ is the sector dependent azimuthal angle, with $\phi = 0$ corresponding to the center of the sector.

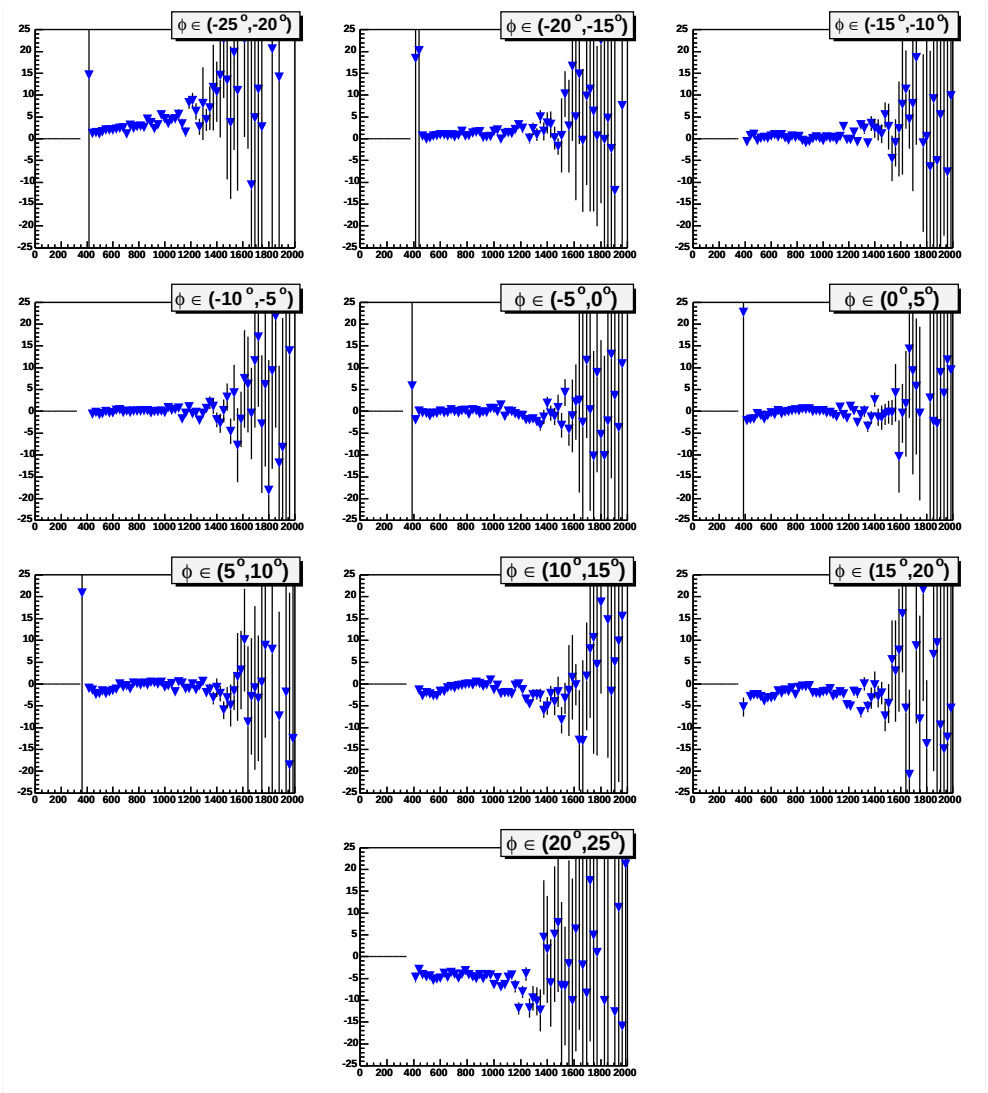

Figure 20: $\Delta\frac{Bdl}{p}$ vs. $\frac{Bdl}{p}$: The change in $\frac{Bdl}{p}$, for the π^-, in Sector 3. $\frac{Bdl}{p}$ has units of $\frac{kG\cdot cm}{GeV}$ and ϕ is the sector dependent azimuthal angle, with $\phi = 0$ corresponding to the center of the sector.

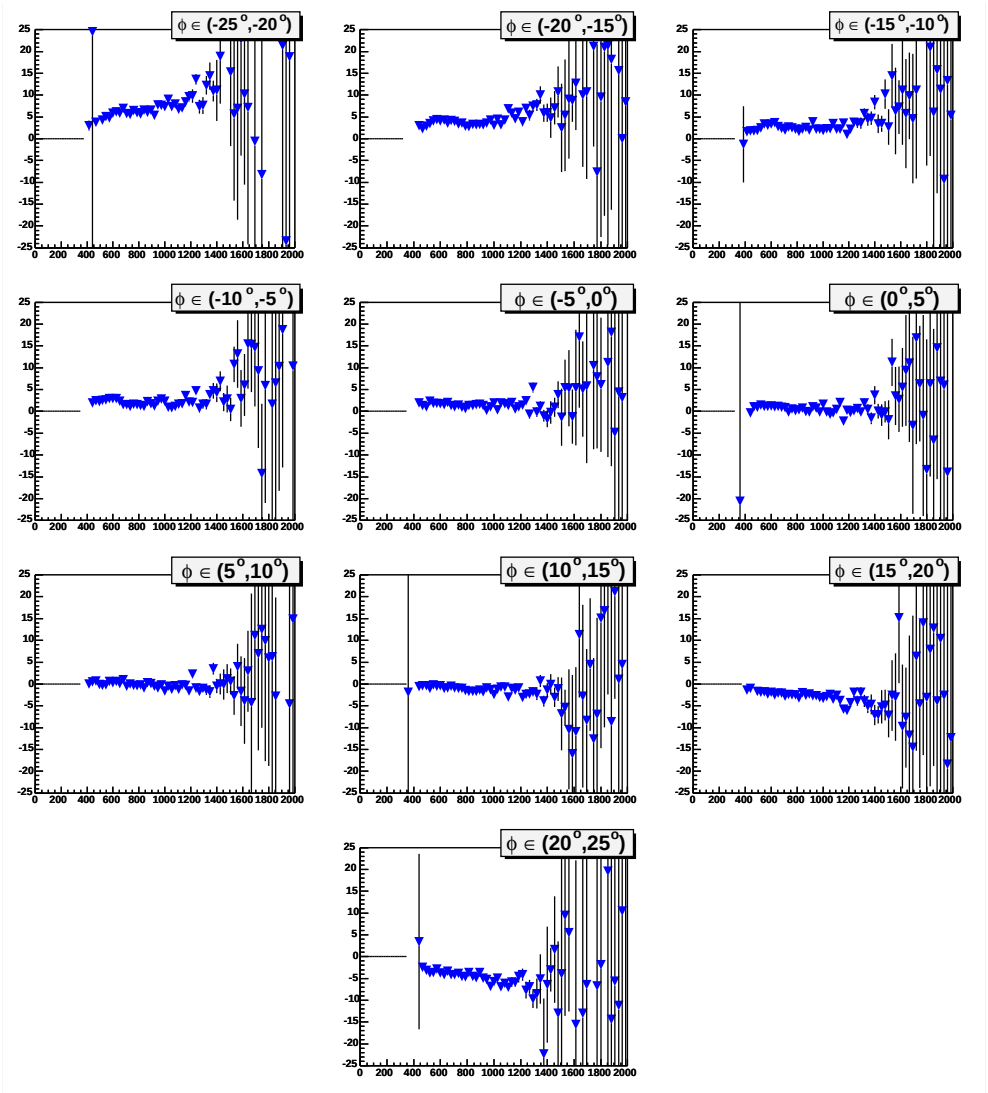

Figure 21: $\Delta\frac{Bdl}{p}$ vs. $\frac{Bdl}{p}$: The change in $\frac{Bdl}{p}$, for the π^-, in Sector 4. $\frac{Bdl}{p}$ has units of $\frac{kG \cdot cm}{GeV}$ and ϕ is the sector dependent azimuthal angle, with $\phi = 0$ corresponding to the center of the sector.

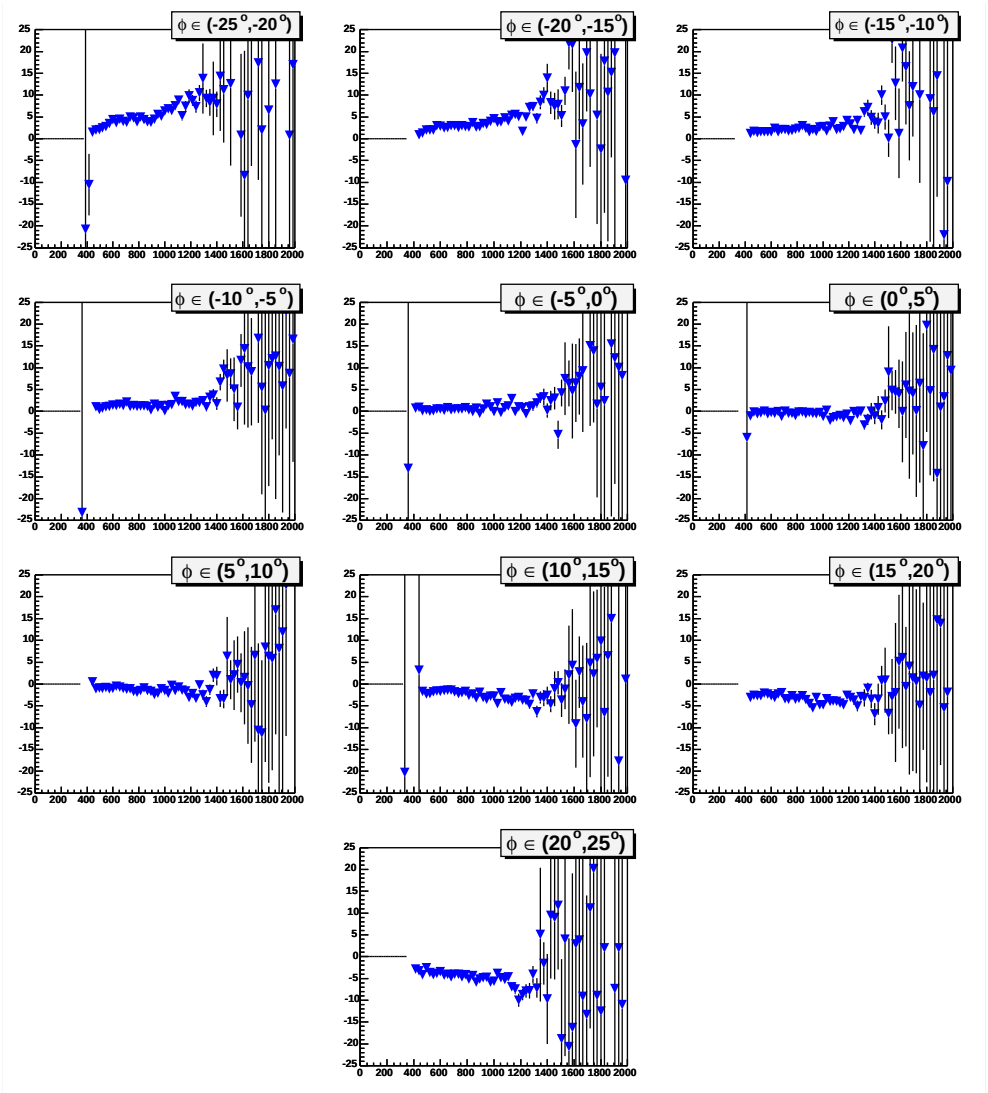

Figure 22: $\Delta\frac{Bdl}{p}$ vs. $\frac{Bdl}{p}$: The change in $\frac{Bdl}{p}$, for the π^-, in Sector 5. $\frac{Bdl}{p}$ has units of $\frac{kG\cdot cm}{GeV}$ and ϕ is the sector dependent azimuthal angle, with $\phi = 0$ corresponding to the center of the sector.

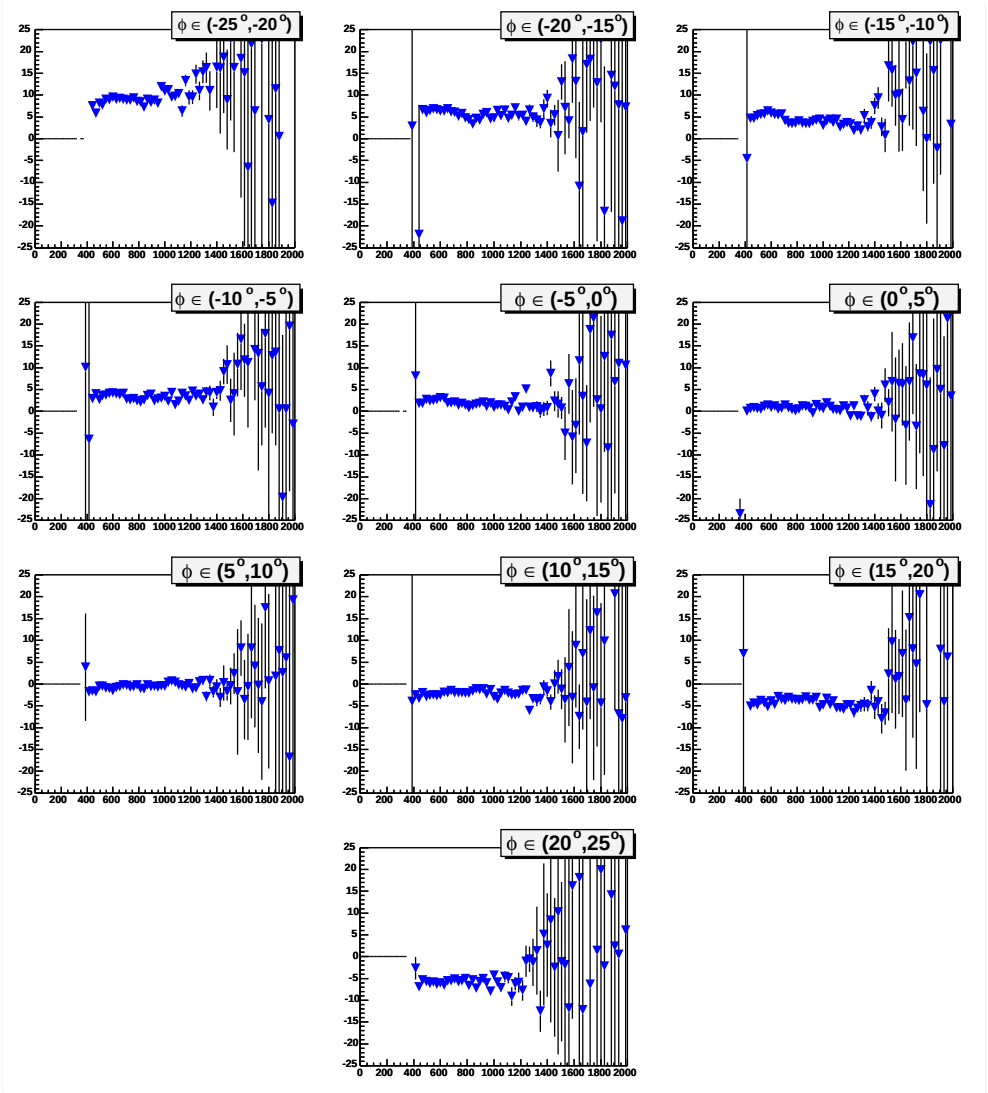

Figure 23: $\Delta\frac{Bdl}{p}$ vs. $\frac{Bdl}{p}$: The change in $\frac{Bdl}{p}$, for the π^-, in Sector 6. $\frac{Bdl}{p}$ has units of $\frac{kG \cdot cm}{GeV}$ and ϕ is the sector dependent azimuthal angle, with $\phi = 0$ corresponding to the center of the sector.

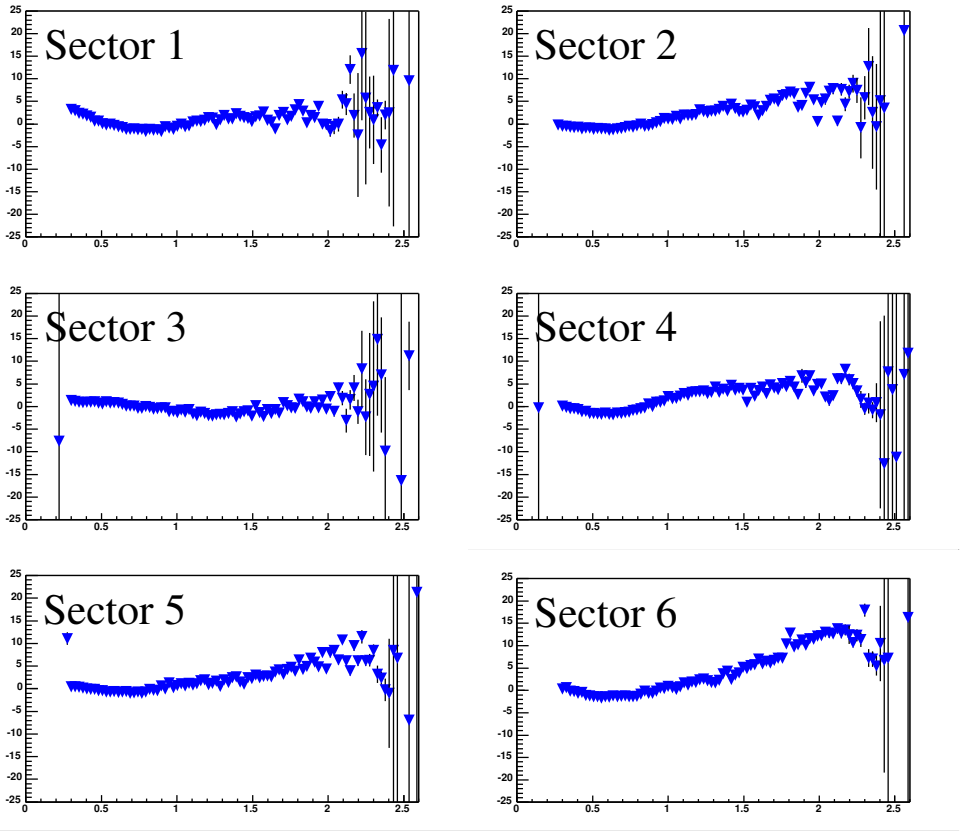

Figure 24: $\Delta\frac{Bdl}{p}$ vs. θ : The change in $\frac{Bdl}{p}$, for the π^-, in each sector as a function of θ. $\frac{Bdl}{p}$ has units of $\frac{kG \cdot cm}{GeV}$.

B π^+ Corrections

This appendix shows detailed plots of the π^+ momentum corrections. Figures 34, 35,36,37,38 and 39 show the quantity $\Delta\frac{Bdl}{p}$ versus $\frac{Bdl}{p}$ in sectors 1-6. The plots are broken into ten bins in ϕ in each sector. Figure 25 shows the corrections made to one run from the g1c data summed over all 6 sectors. The corrections are small, typically only a few MeV.

The π^+ corrections have a decreasing slope, in the $\Delta\frac{Bdl}{p}$ vs. $\frac{Bdl}{p}$ plots, as ϕ increases. Recall that in Appendix A we also saw this affect in the π^- corrections and attributed it to a rotation of the drift chambers with respect to the torus coils. A rotation of the drift chambers would be seen in both postive and negative particles.

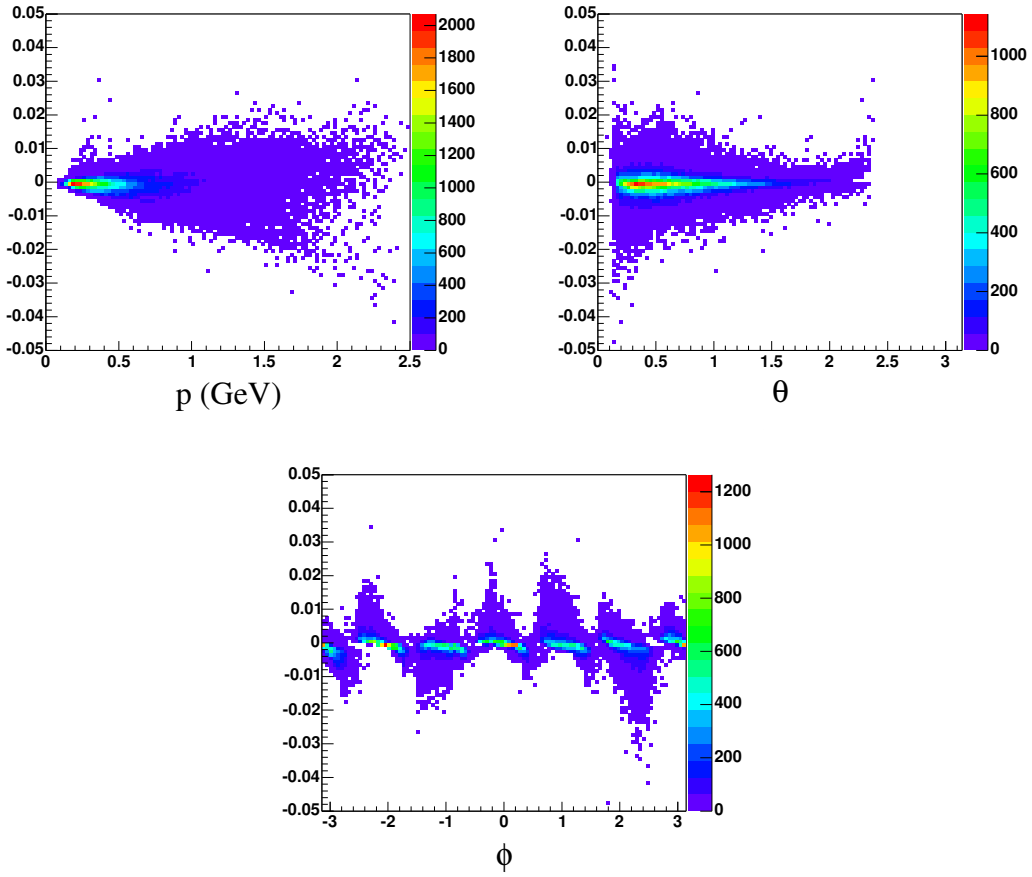

Figure 25: Corrections to the π^+ momentum as a function of p, θ and ϕ summed over all 6 sectors.

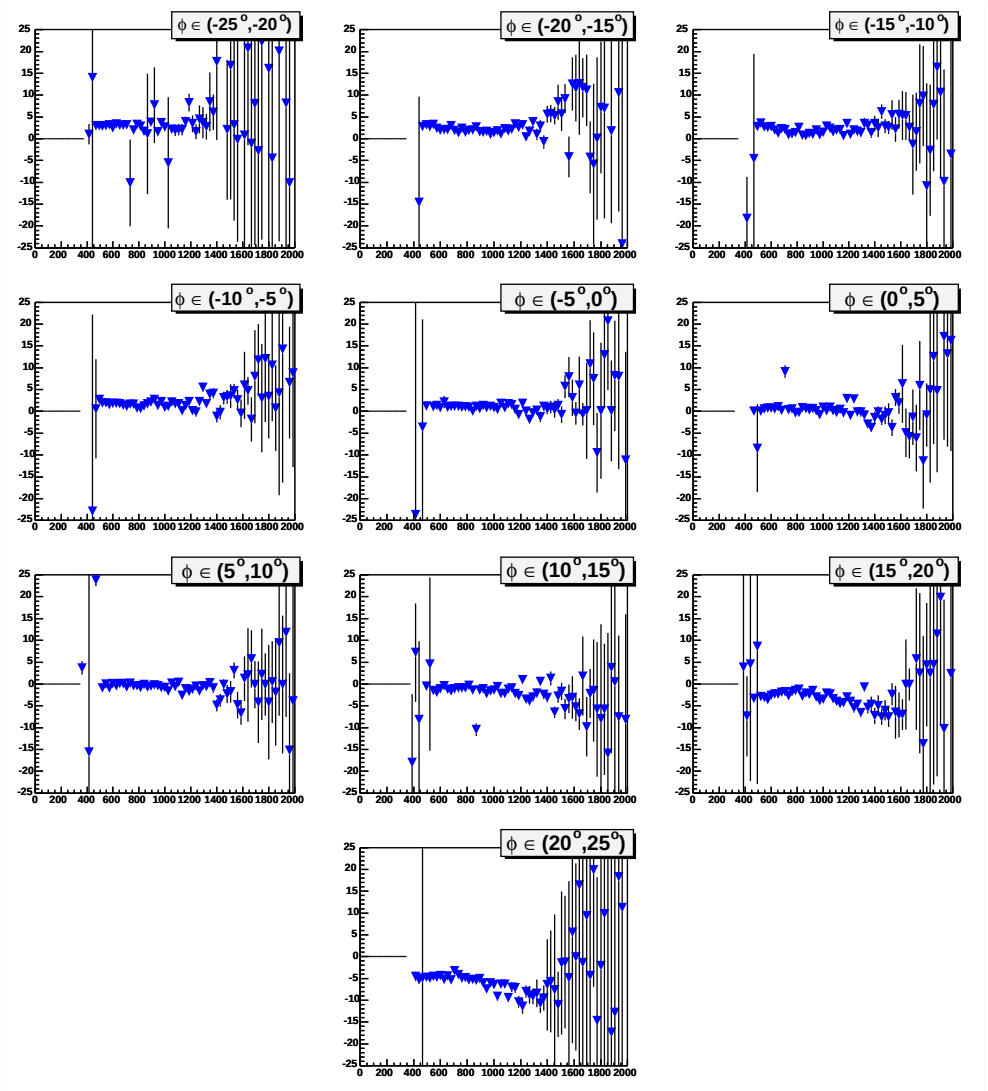

Figure 26: $\Delta\frac{Bdl}{p}$ vs. $\frac{Bdl}{p}$: The change in $\frac{Bdl}{p}$, for the π^+, in Sector 1. $\frac{Bdl}{p}$ has units of $\frac{kG\cdot cm}{GeV}$ and ϕ is the sector dependent azimuthal angle, with $\phi = 0$ corresponding to the center of the sector.

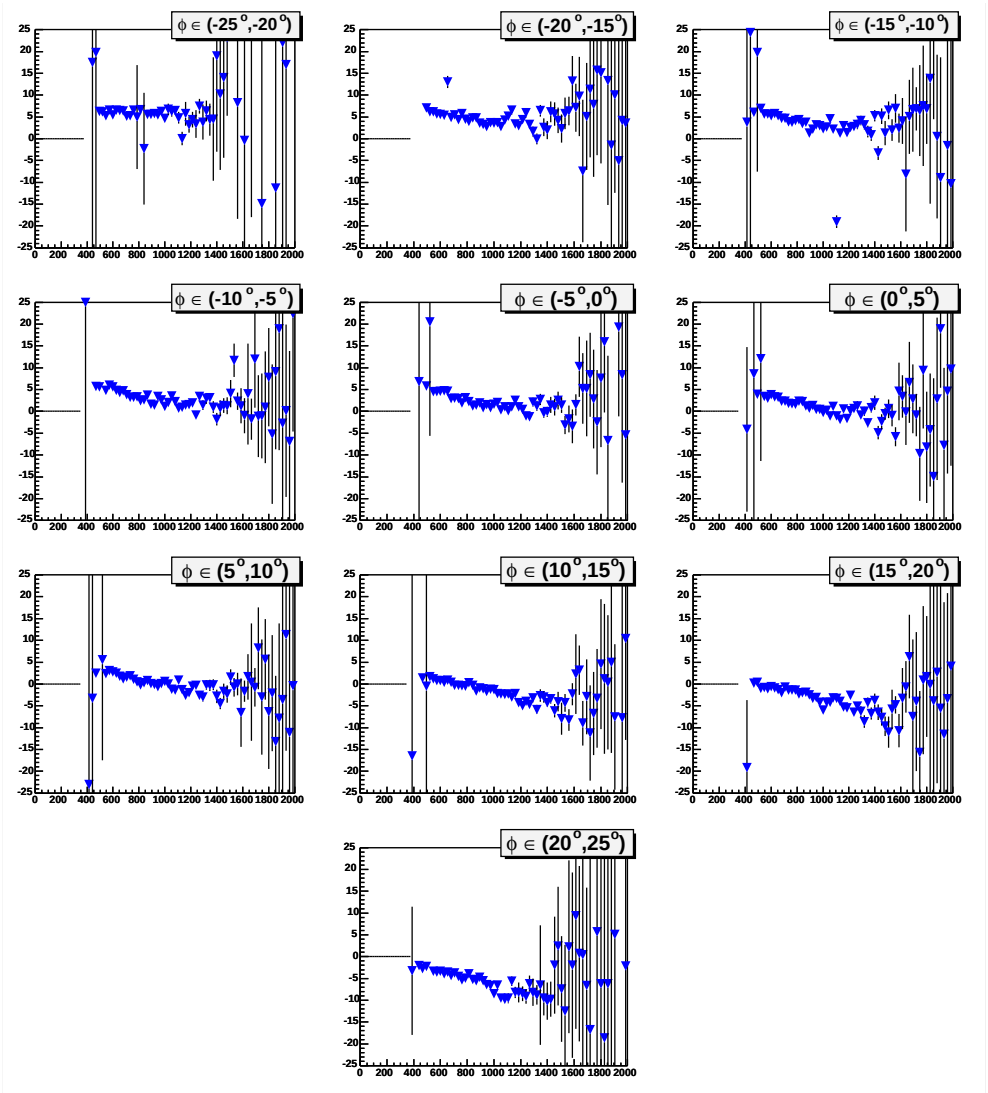

Figure 27: $\Delta\frac{Bdl}{p}$ vs. $\frac{Bdl}{p}$: The change in $\frac{Bdl}{p}$, for the π^+, in Sector 2. $\frac{Bdl}{p}$ has units of $\frac{kG \cdot cm}{GeV}$ and ϕ is the sector dependent azimuthal angle, with $\phi = 0$ corresponding to the center of the sector.

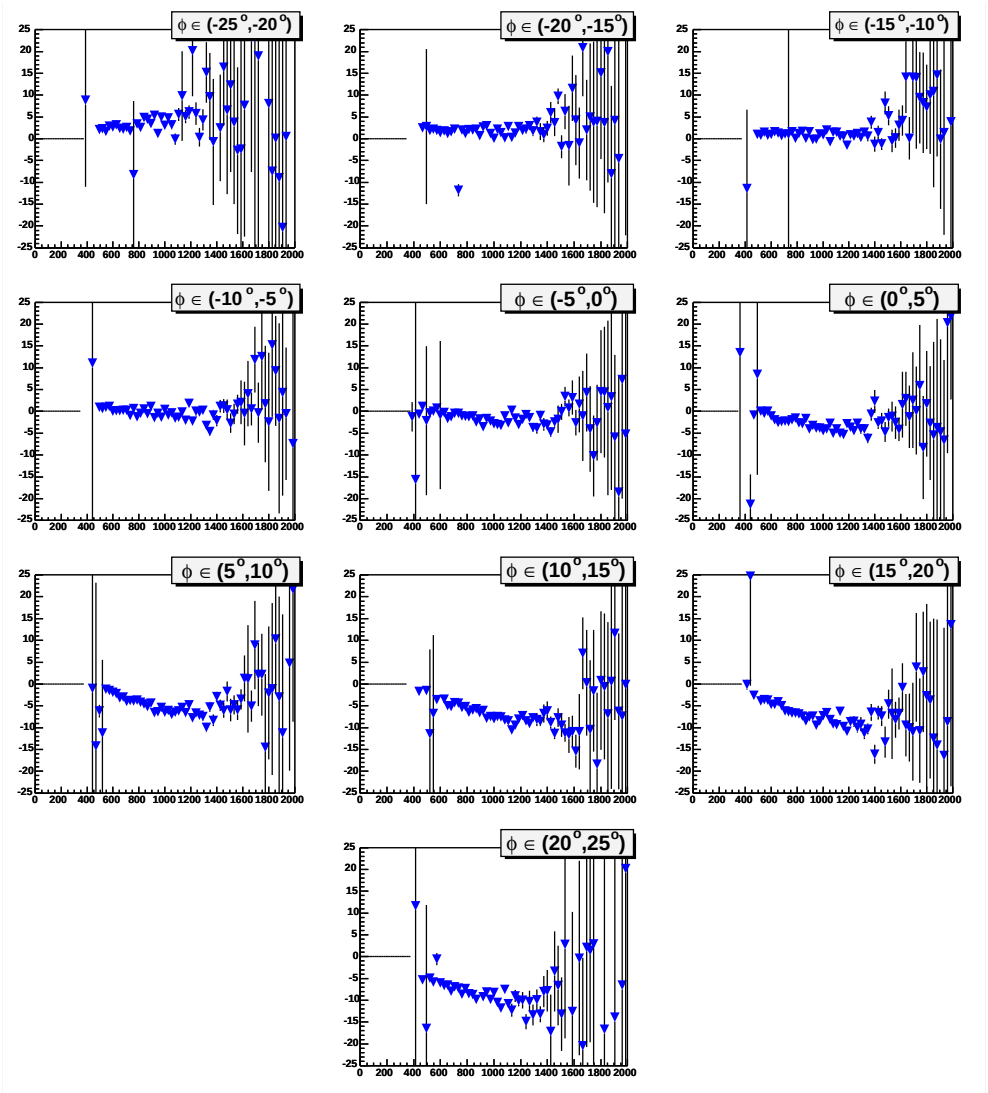

Figure 28: $\Delta\frac{Bdl}{p}$ vs. $\frac{Bdl}{p}$: The change in $\frac{Bdl}{p}$, for the π^+, in Sector 3. $\frac{Bdl}{p}$ has units of $\frac{kG\cdot cm}{GeV}$ and ϕ is the sector dependent azimuthal angle, with $\phi = 0$ corresponding to the center of the sector.

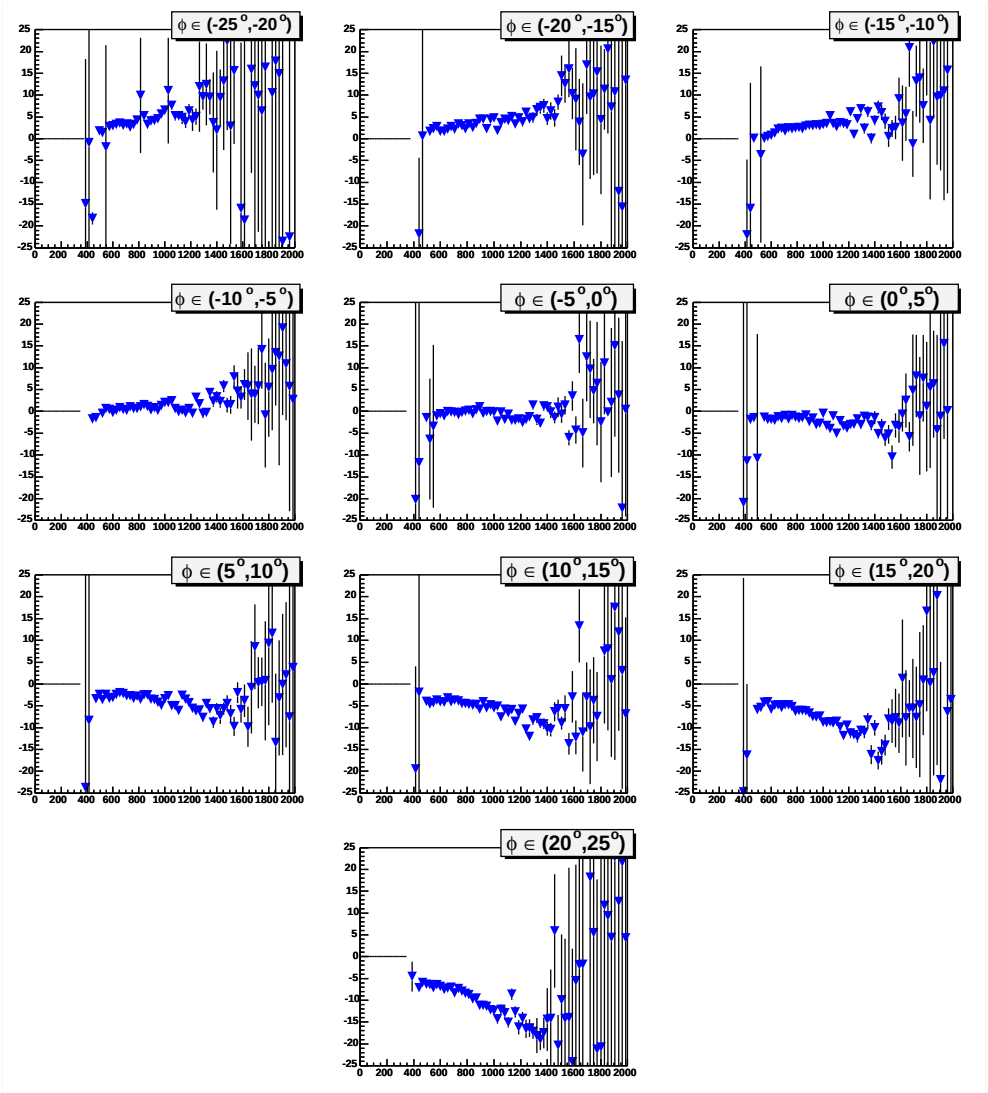

Figure 29: $\Delta\frac{Bdl}{p}$ vs. $\frac{Bdl}{p}$: The change in $\frac{Bdl}{p}$, for the π^+, in Sector 4. $\frac{Bdl}{p}$ has units of $\frac{kG \cdot cm}{GeV}$ and ϕ is the sector dependent azimuthal angle, with $\phi = 0$ corresponding to the center of the sector.

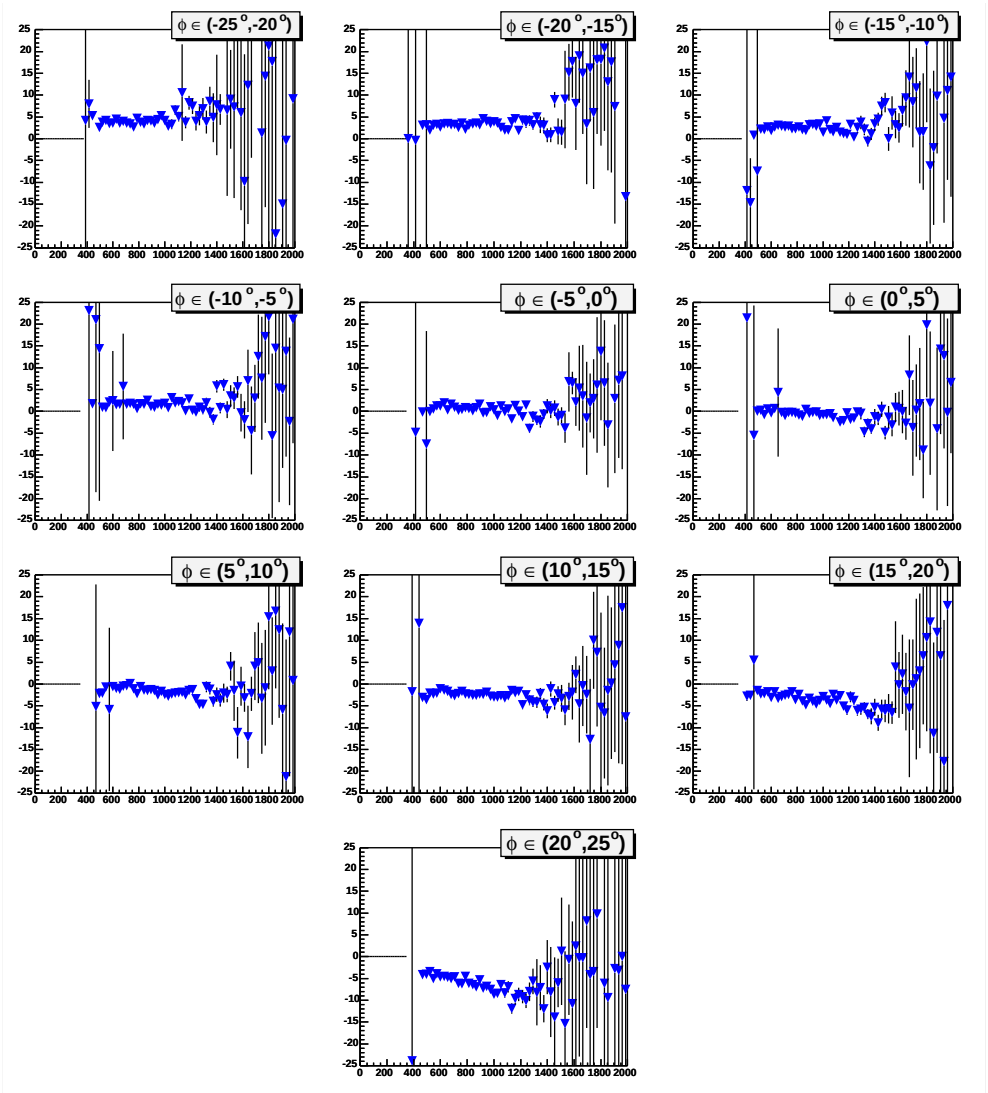

Figure 30: $\Delta\frac{Bdl}{p}$ vs. $\frac{Bdl}{p}$: The change in $\frac{Bdl}{p}$, for the π^+, in Sector 5. $\frac{Bdl}{p}$ has units of $\frac{kG\cdot cm}{GeV}$ and ϕ is the sector dependent azimuthal angle, with $\phi = 0$ corresponding to the center of the sector.

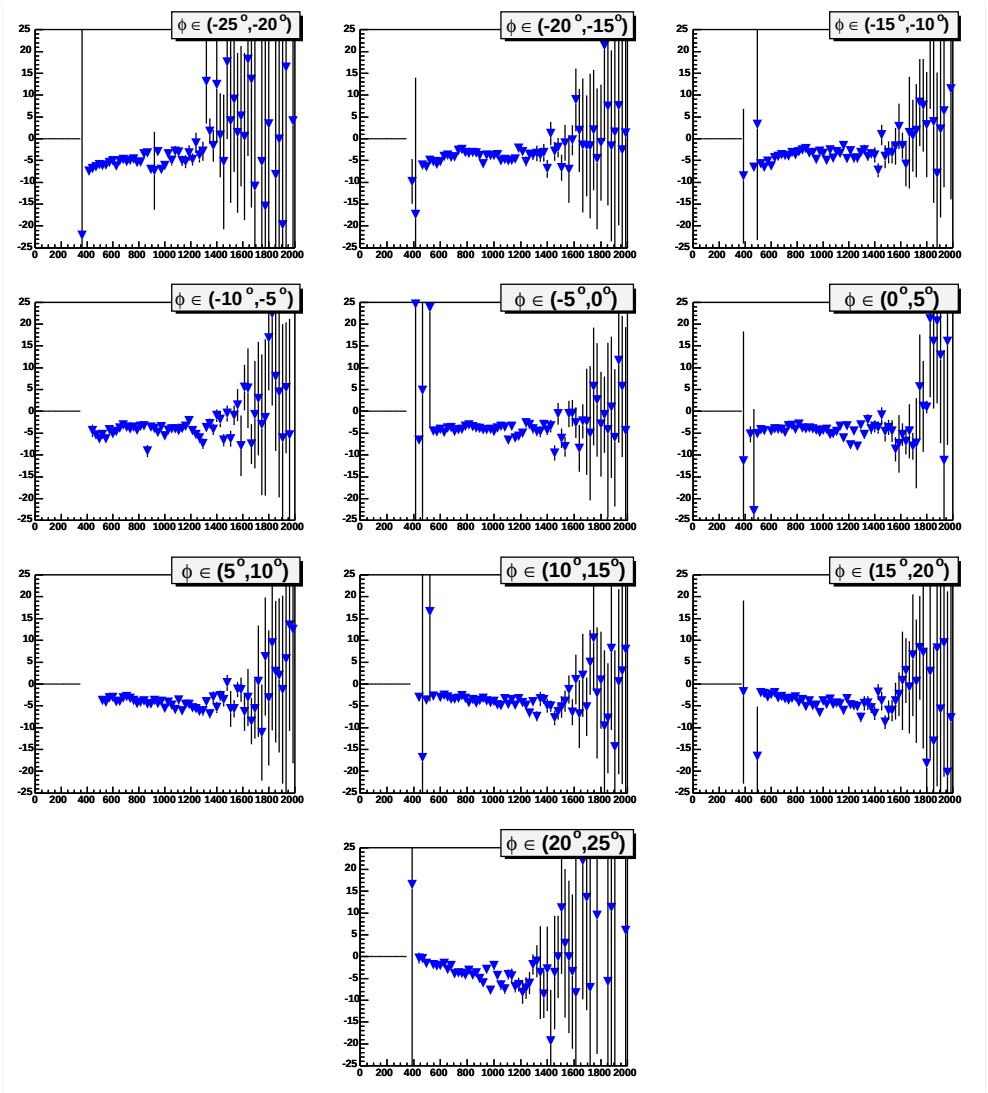

Figure 31: $\Delta\frac{Bdl}{p}$ vs. $\frac{Bdl}{p}$: The change in $\frac{Bdl}{p}$, for the π^+, in Sector 6. $\frac{Bdl}{p}$ has units of $\frac{kG \cdot cm}{GeV}$ and ϕ is the sector dependent azimuthal angle, with $\phi = 0$ corresponding to the center of the sector.

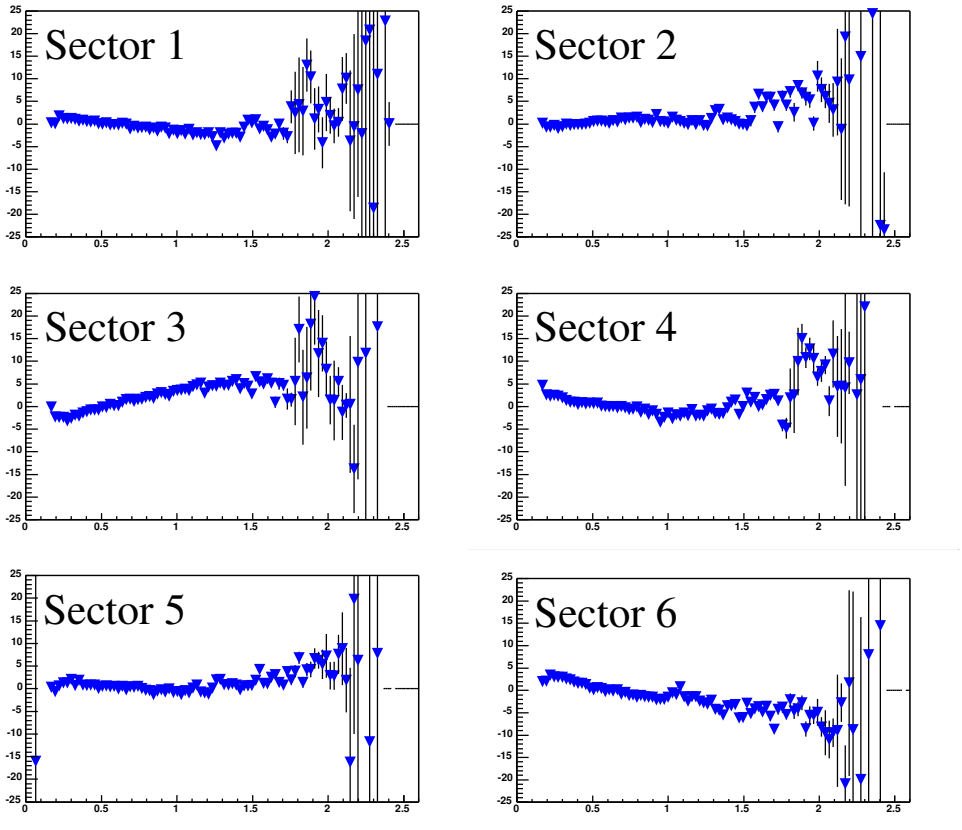

Figure 32: $\Delta\frac{Bdl}{p}$ vs. θ : The change in $\frac{Bdl}{p}$, for the π^+, in each sector as a function of θ. $\frac{Bdl}{p}$ has units of $\frac{kG \cdot cm}{GeV}$.

C Applying the π^+ corrections to the proton

The plots in this appendix show the affects of applying the π^+ corrections along with the extra eloss correction to the proton. Figures 34, 35,36,37,38 and 39 show the quantity $\Delta\frac{Bdl}{p}$ versus $\frac{Bdl}{p}$ in sectors 1-6. The plots are broken into ten bins in ϕ in each sector. The red circles were calculated using the measured momentum with the standard eloss correction applied. The blue triangles were calculated after applying the π^+ corrections to the proton momentum and using the increased eloss correction. These corrections work quite well, in almost every bin $\Delta\frac{Bdl}{p}$ is consistent with zero. Figure 33 shows the results of applying the π^+ momentum corrections along with the increase to the ELOSS correction (not the correction itself, just the extra $\approx 18\%$) to the proton momentum for one run in the g1c data. Except for protons with mometum less than about 300 MeV/c^2, these corrections are small, typically less than 5 MeV/c^2.

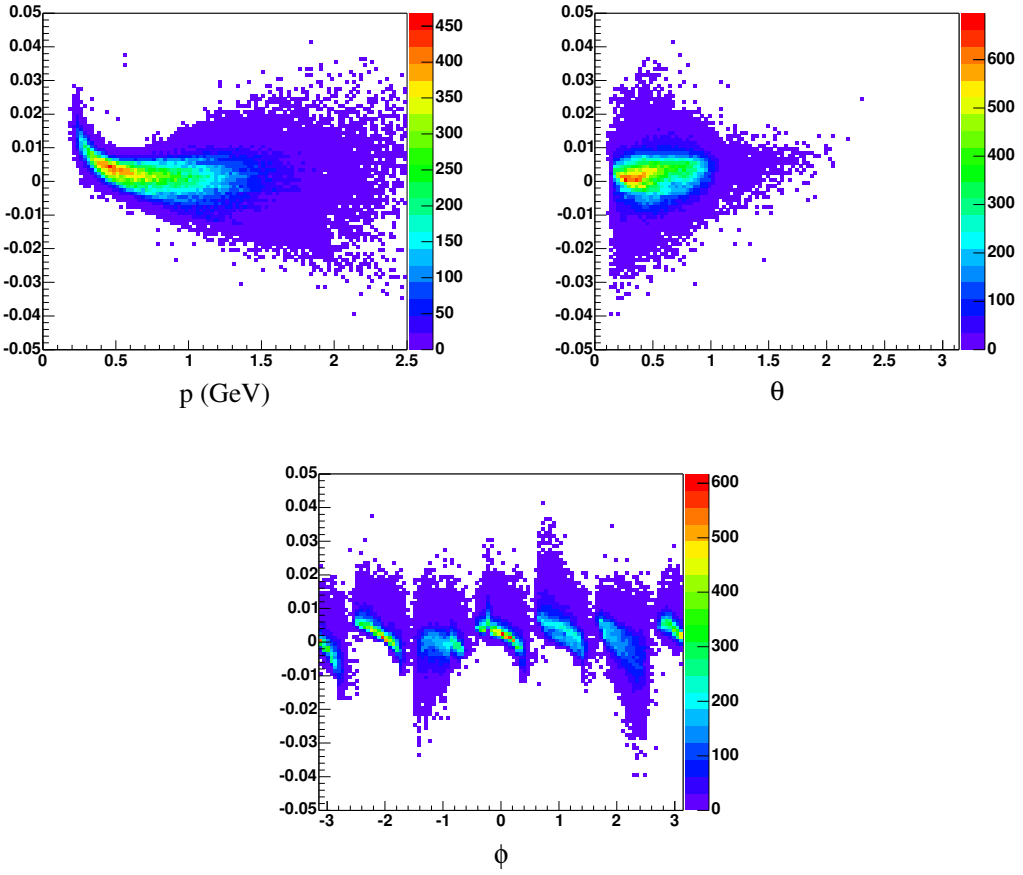

Figure 33: Corrections, including our increase to the eloss correction (but not the standard ELOSS correction), to the proton momentum as a function of p, θ and ϕ summed over all 6 sectors.

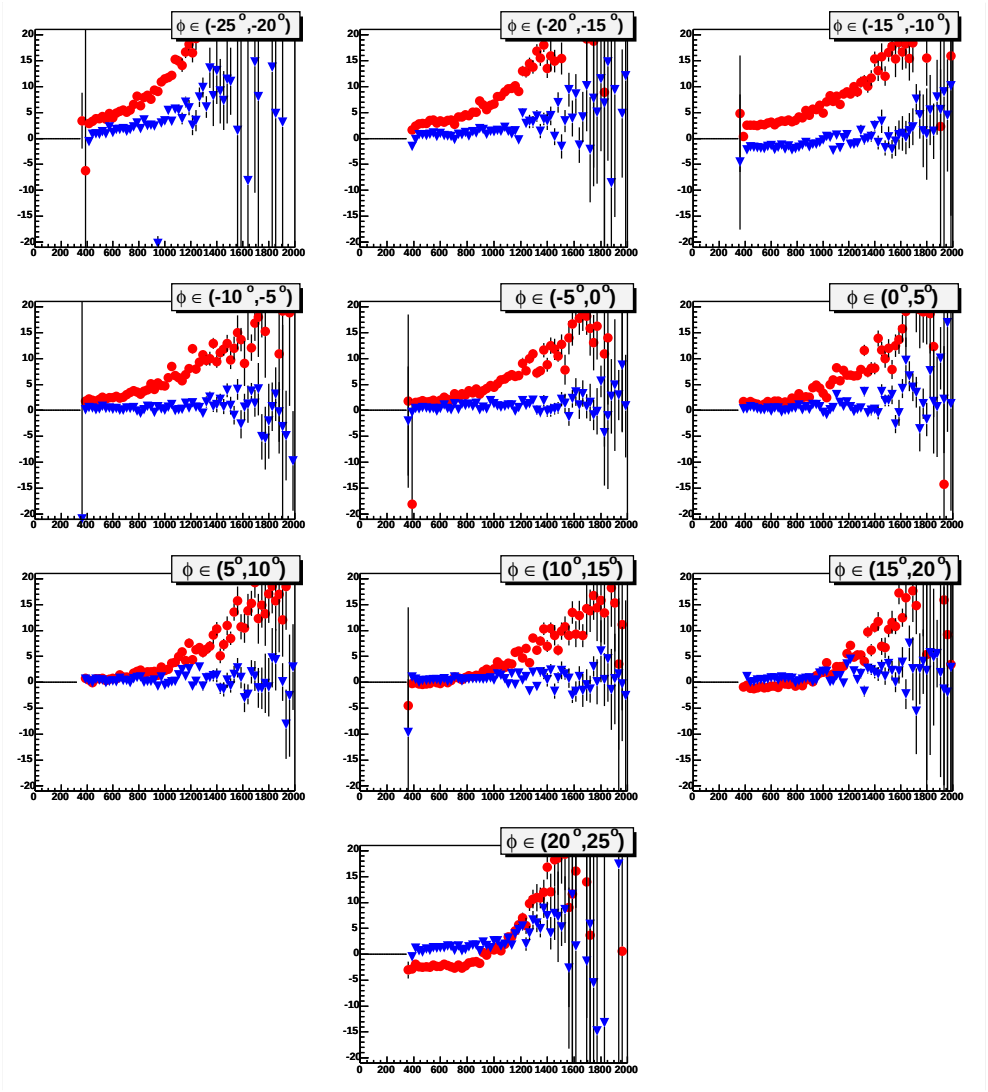

Figure 34: $\Delta\frac{Bdl}{p}$ vs. $\frac{Bdl}{p}$: The change in $\frac{Bdl}{p}$, for the proton, in Sector 1. $\frac{Bdl}{p}$ has units of $\frac{kG \cdot cm}{GeV}$ and ϕ is the sector dependent azimuthal angle, with $\phi = 0$ corresponding to the center of the sector. The red circles were calculated using the measured momentum with the standard eloss correction. The blue triangles were calculated after applying the π^+ momentum corrections to the proton and using the increased eloss correction.

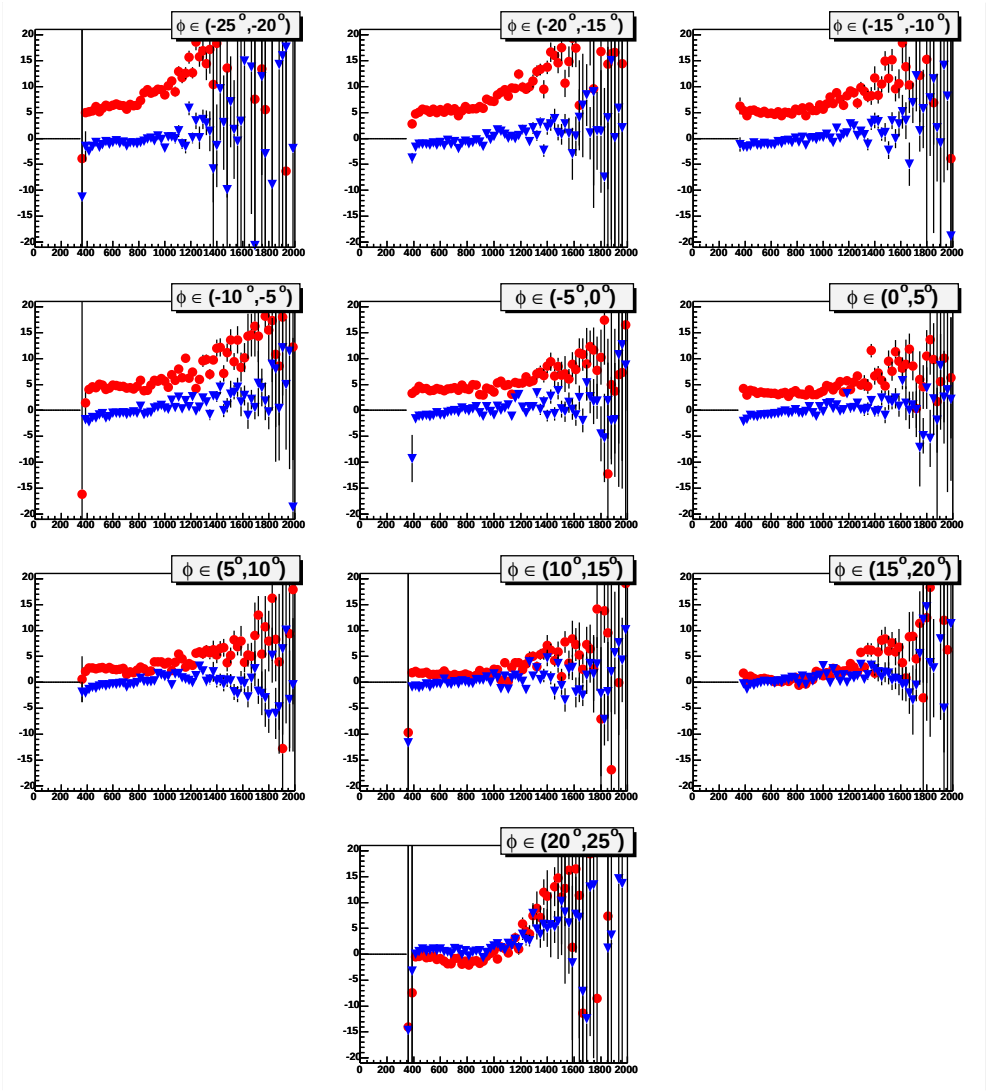

Figure 35: $\Delta\frac{Bdl}{p}$ vs. $\frac{Bdl}{p}$: The change in $\frac{Bdl}{p}$, for the proton, in Sector 2. $\frac{Bdl}{p}$ has units of $\frac{kG \cdot cm}{GeV}$ and ϕ is the sector dependent azimuthal angle, with $\phi = 0$ corresponding to the center of the sector. The red circles were calculated using the measured momentum with the standard eloss correction. The blue triangles were calculated after applying the π^+ momentum corrections to the proton and using the increased eloss correction.

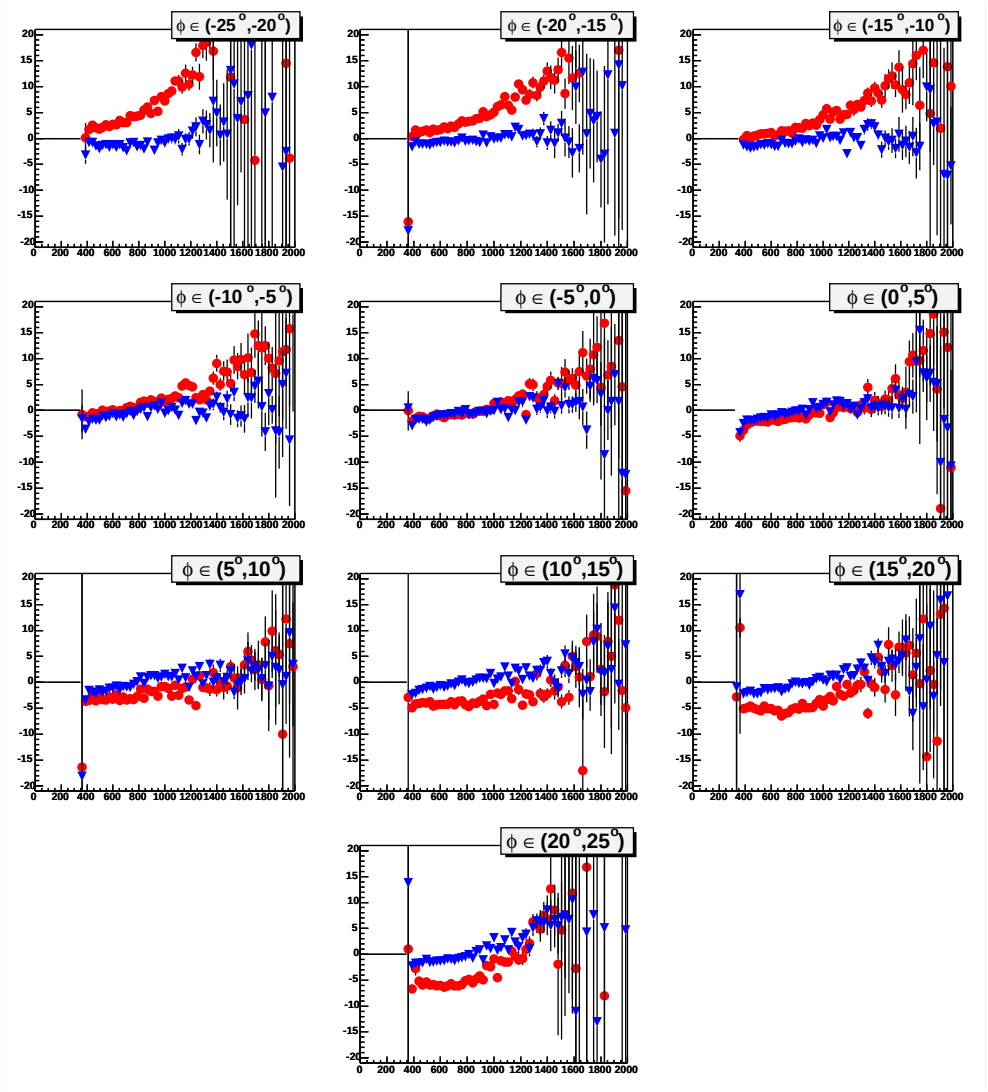

Figure 36: $\Delta\frac{Bdl}{p}$ vs. $\frac{Bdl}{p}$: The change in $\frac{Bdl}{p}$, for the proton, in Sector 3. $\frac{Bdl}{p}$ has units of $\frac{kG \cdot cm}{GeV}$ and ϕ is the sector dependent azimuthal angle, with $\phi = 0$ corresponding to the center of the sector. The red circles were calculated using the measured momentum with the standard eloss correction. The blue triangles were calculated after applying the π^+ momentum corrections to the proton and using the increased eloss correction.

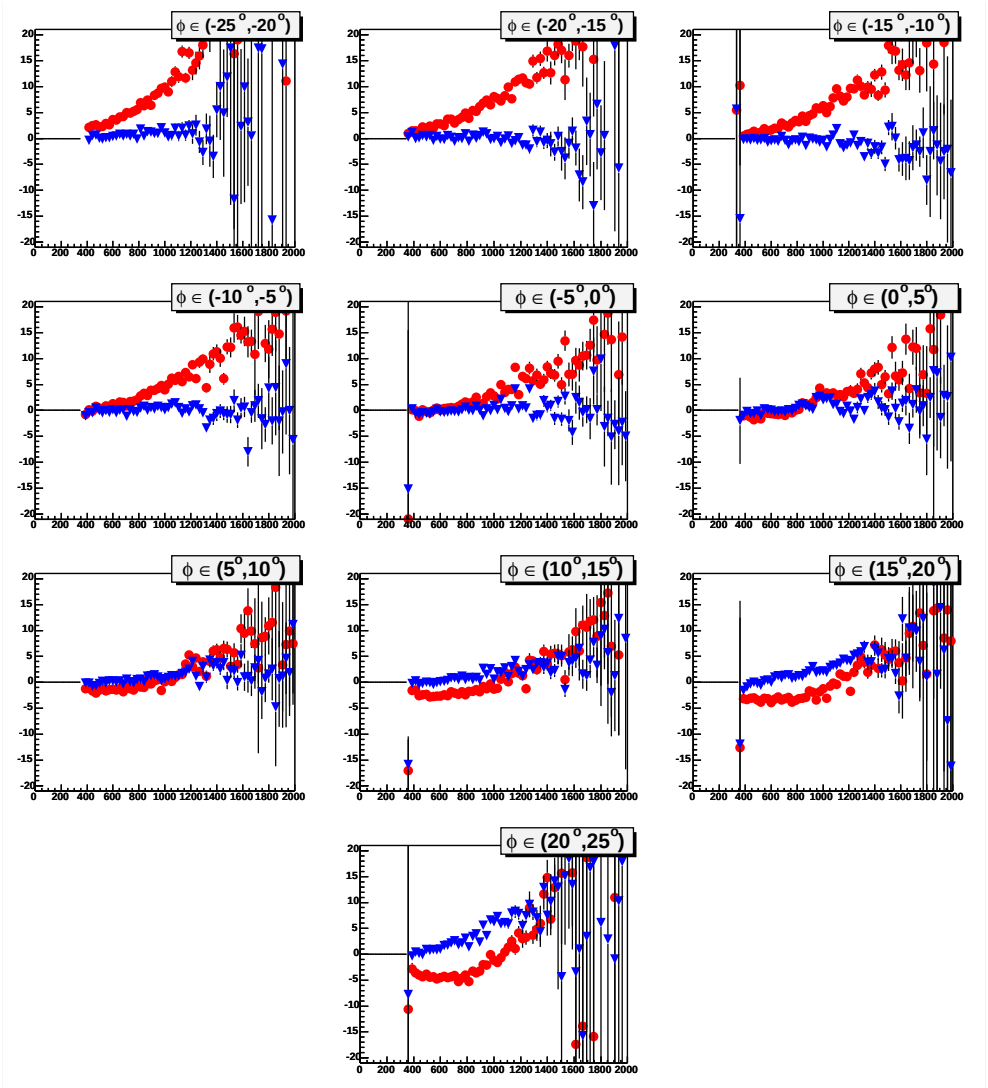

Figure 37: $\Delta\frac{Bdl}{p}$ vs. $\frac{Bdl}{p}$: The change in $\frac{Bdl}{p}$, for the proton, in Sector 4. $\frac{Bdl}{p}$ has units of $\frac{kG \cdot cm}{GeV}$ and ϕ is the sector dependent azimuthal angle, with $\phi = 0$ corresponding to the center of the sector. The red circles were calculated using the measured momentum with the standard eloss correction. The blue triangles were calculated after applying the π^+ momentum corrections to the proton and using the increased eloss correction.

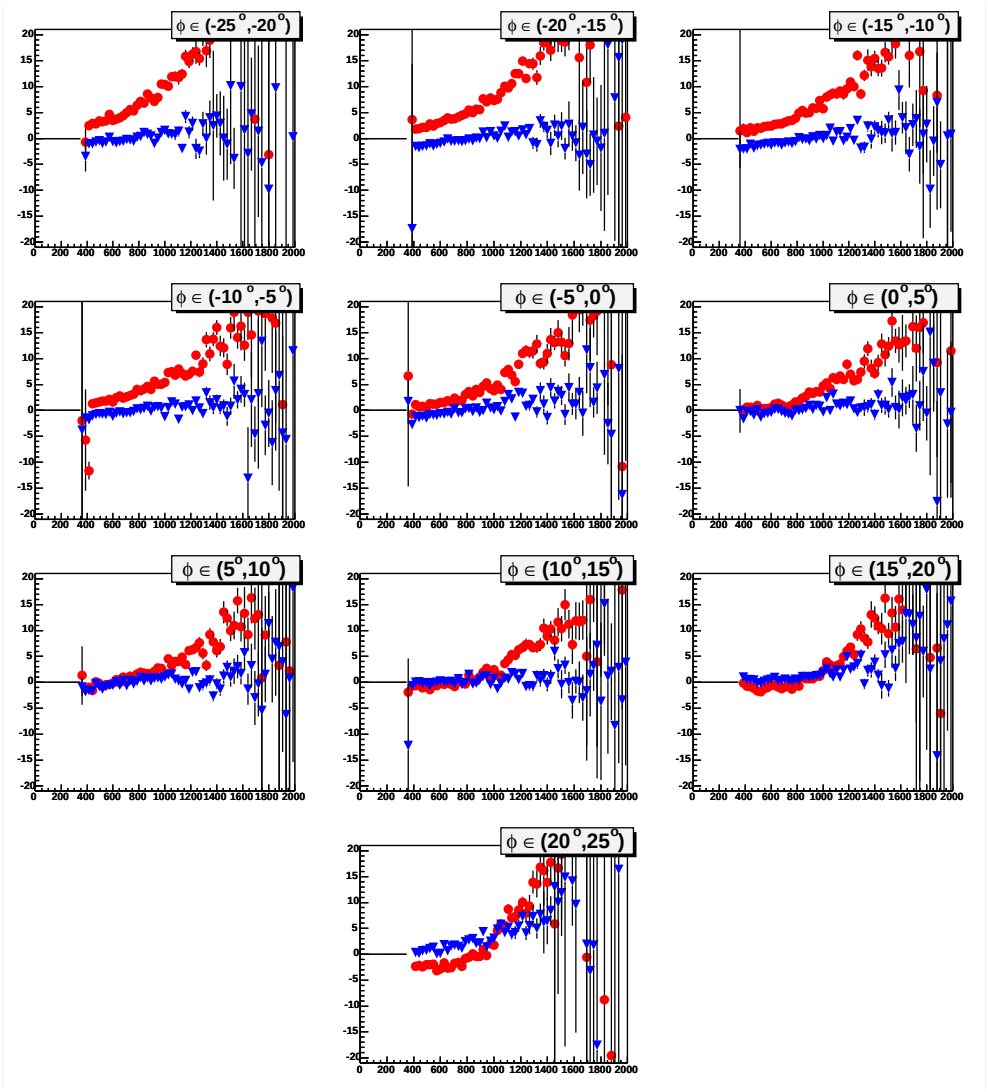

Figure 38: $\Delta\frac{Bdl}{p}$ vs. $\frac{Bdl}{p}$: The change in $\frac{Bdl}{p}$, for the proton, in Sector 5. $\frac{Bdl}{p}$ has units of $\frac{kG \cdot cm}{GeV}$ and ϕ is the sector dependent azimuthal angle, with $\phi = 0$ corresponding to the center of the sector. The red circles were calculated using the measured momentum with the standard eloss correction. The blue triangles were calculated after applying the π^+ momentum corrections to the proton and using the increased eloss correction.

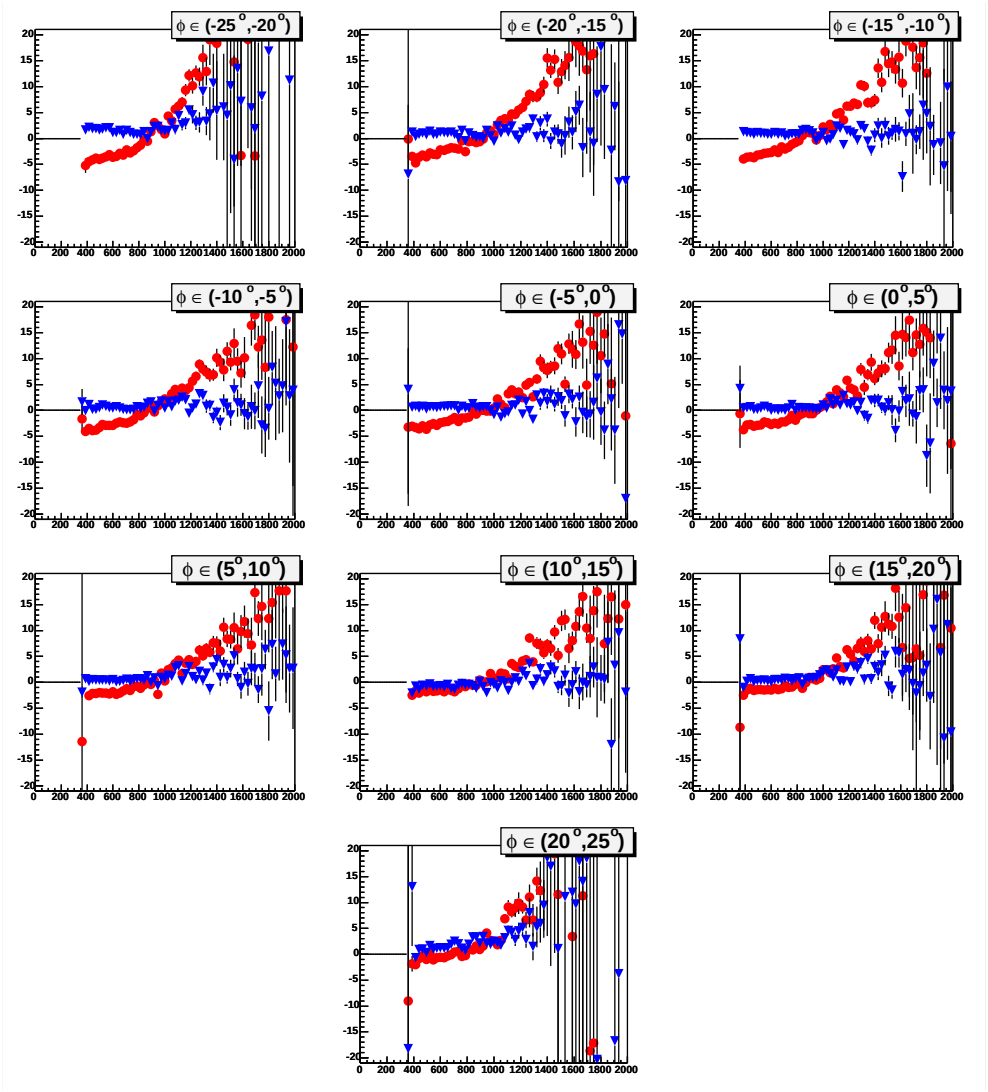

Figure 39: $\Delta\frac{Bdl}{p}$ vs. $\frac{Bdl}{p}$: The change in $\frac{Bdl}{p}$, for the proton, in Sector 6. $\frac{Bdl}{p}$ has units of $\frac{kG \cdot cm}{GeV}$ and ϕ is the sector dependent azimuthal angle, with $\phi = 0$ corresponding to the center of the sector. The red circles were calculated using the measured momentum with the standard eloss correction. The blue triangles were calculated after applying the π^+ momentum corrections to the proton and using the increased eloss correction.

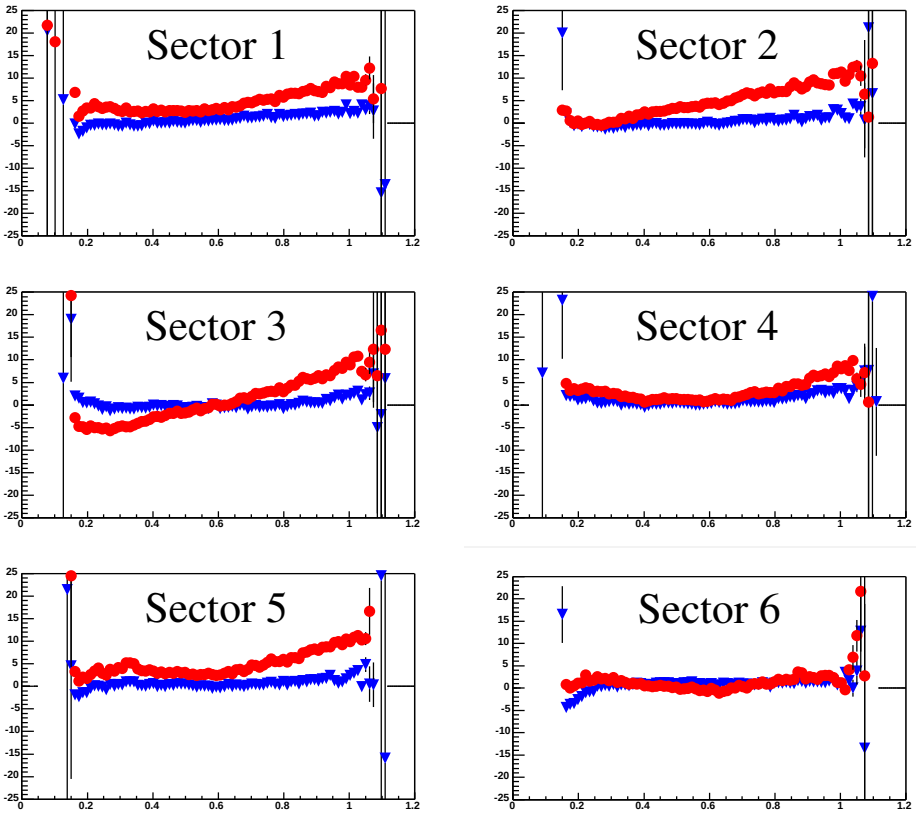

Figure 40: $\Delta\frac{Bdl}{p}$ vs. θ : The change in $\frac{Bdl}{p}$, for the proton, in each sector as a function of θ. $\frac{Bdl}{p}$ has units of $\frac{kG\cdot cm}{GeV}$. The red circles were calculated using the measured momentum with the standard eloss correction. The blue triangles were calculated after applying the π^+ momentum corrections to the proton and using the increased eloss correction.